

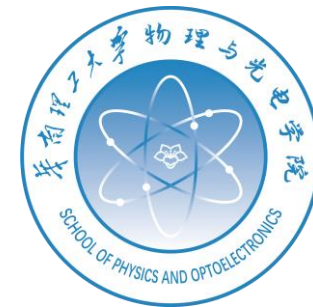
Extracting the high-density symmetry energy with pion and subthreshold hyperon production in heavy-ion collisions

Zhao-Qing Feng*

South China University of Technology, Guangzhou

***Email: fengzhq@scut.edu.cn**

Collaborators: Si-Na Wei, Hui-Gan Cheng, Heng-Jin Liu, Ban Zhang



OUTLINE

- **Neutron star matter and observables in heavy-ion collisions (HICs)**
- **Transport approach for symmetry energy (LQMD)**
- **Results and discussion**
 - **Nuclear cluster and hypernuclide production**
 - **π^-/π^+ ratio for constraining the high-density symmetry energy**
 - **Subthreshold hyperon production in heavy-ion collisions**
- **Summary and perspective**

I. Neutron star matter and pion probes in heavy-ion collisions



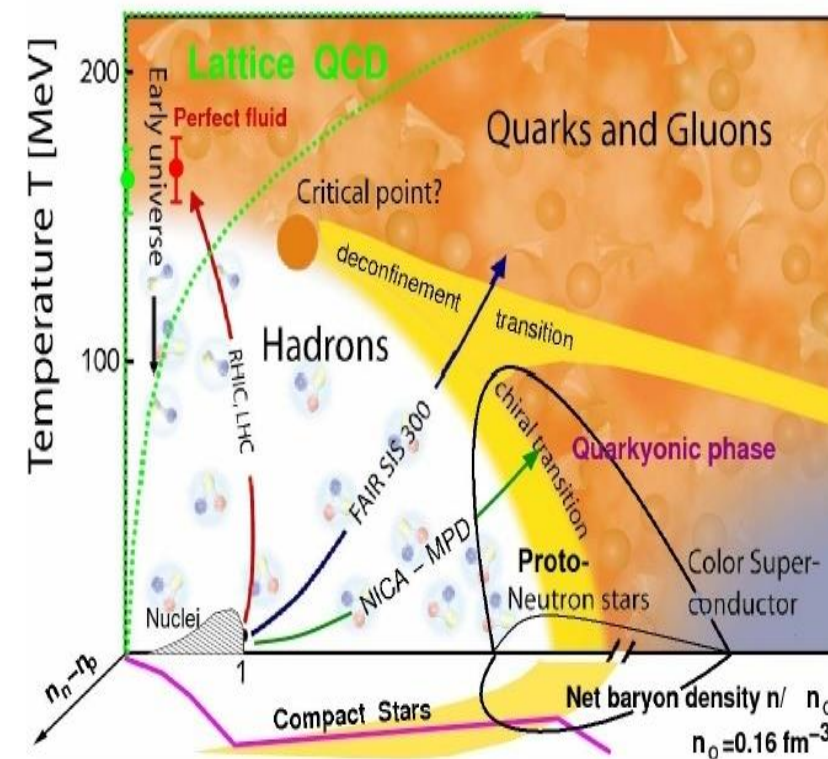
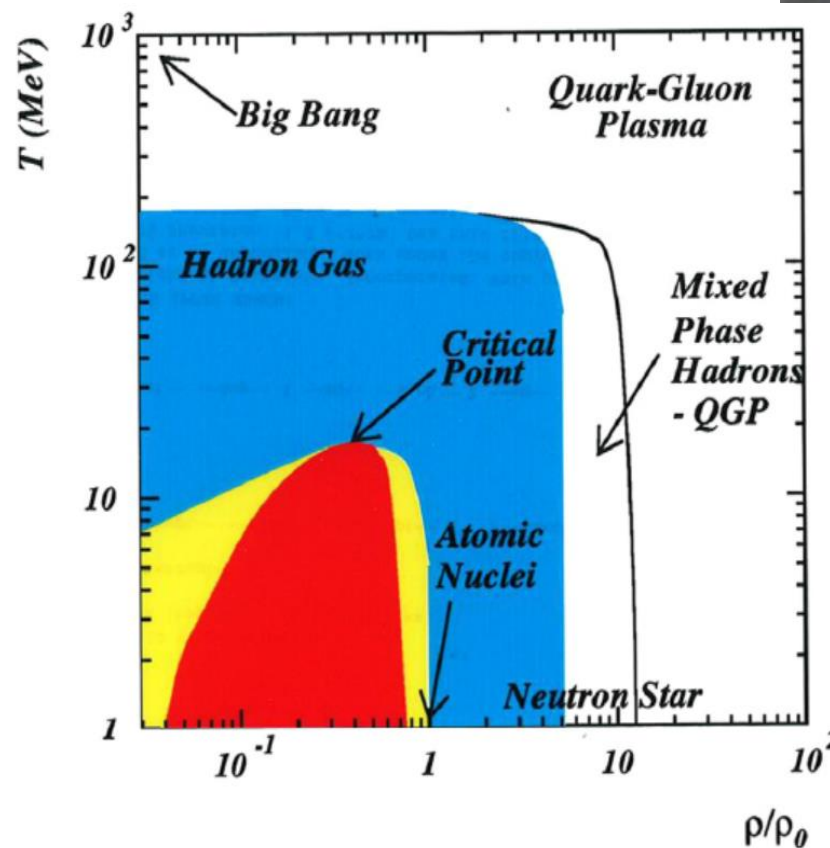
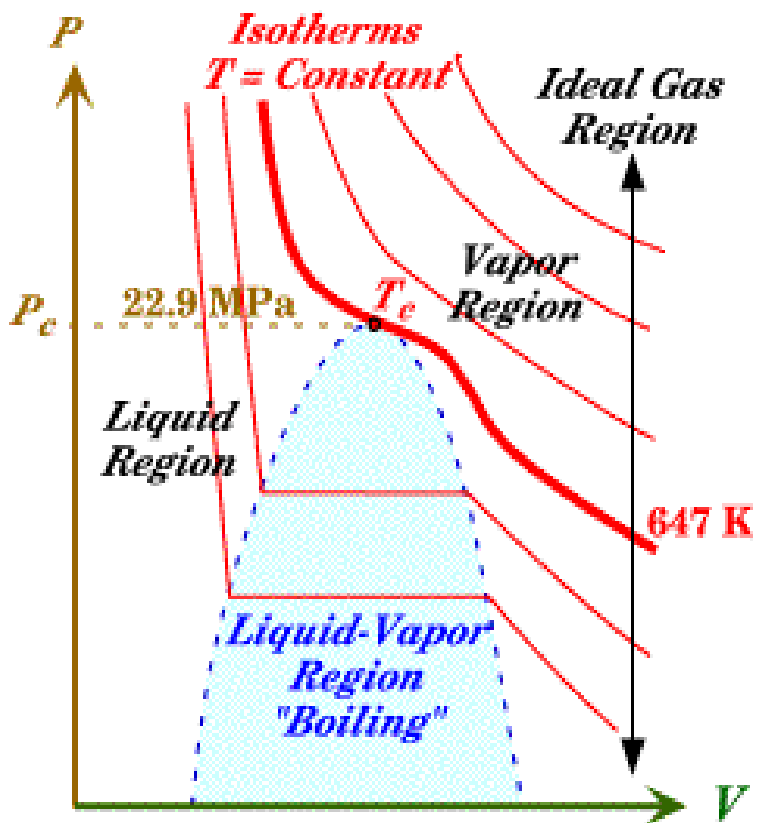
EOS-Equation of State

Van der Waals equation
$$\left[p + a\left(\frac{n}{V}\right)^2 \right] (v - nb) = nRT$$



Johannes Diderik van der Waals
1837- 1923

Nobel Laureate in physics 1910
for study of gas and liquid
equation of state



Nuclear symmetry energy

$$E_{\text{sym}}(\rho) = E_{\text{sym}}(\rho_0) + \frac{L}{3} \left(\frac{\rho - \rho_0}{\rho_0} \right) + \frac{K_{\text{sym}}}{18} \left(\frac{\rho - \rho_0}{\rho_0} \right)^2,$$

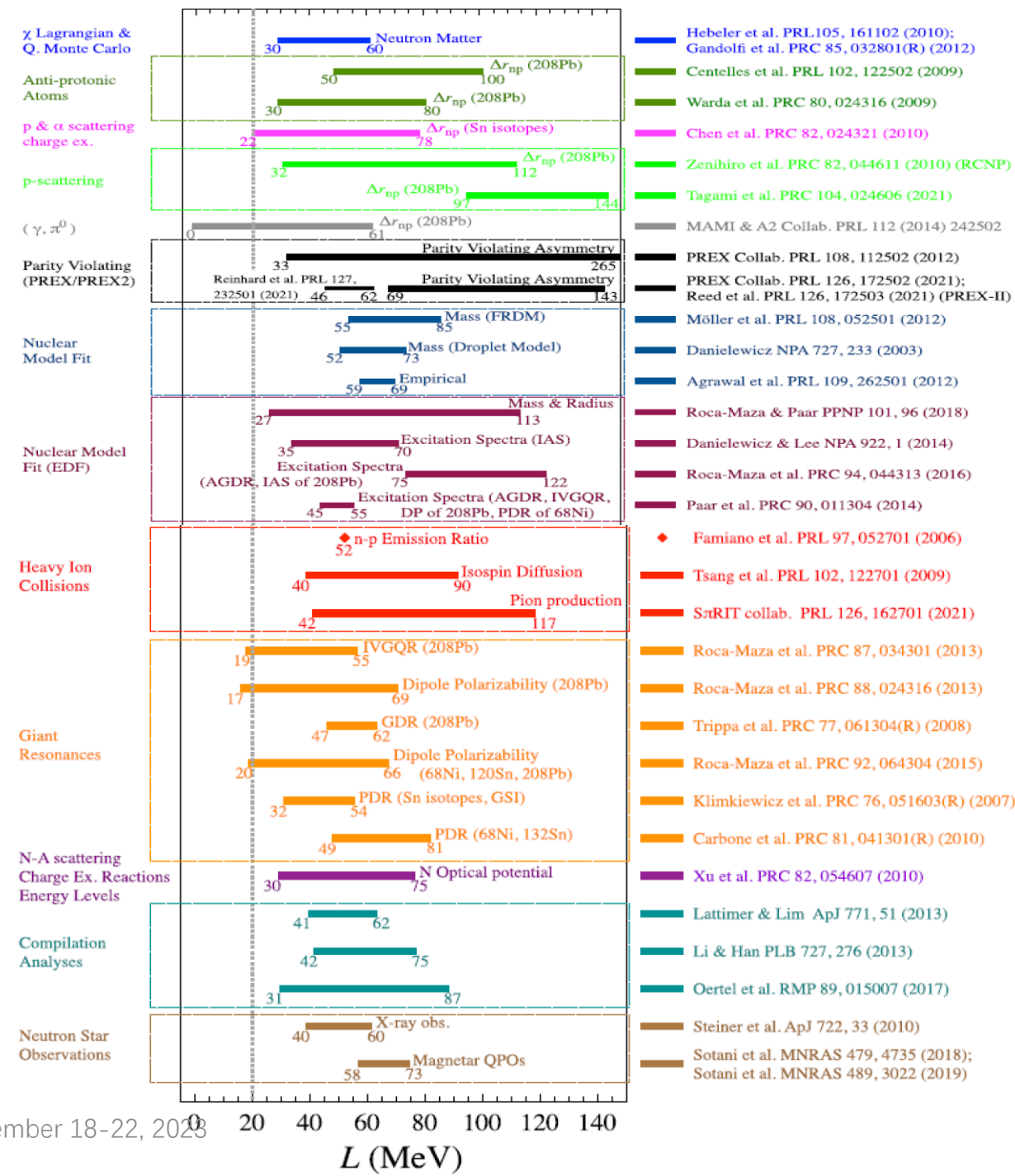
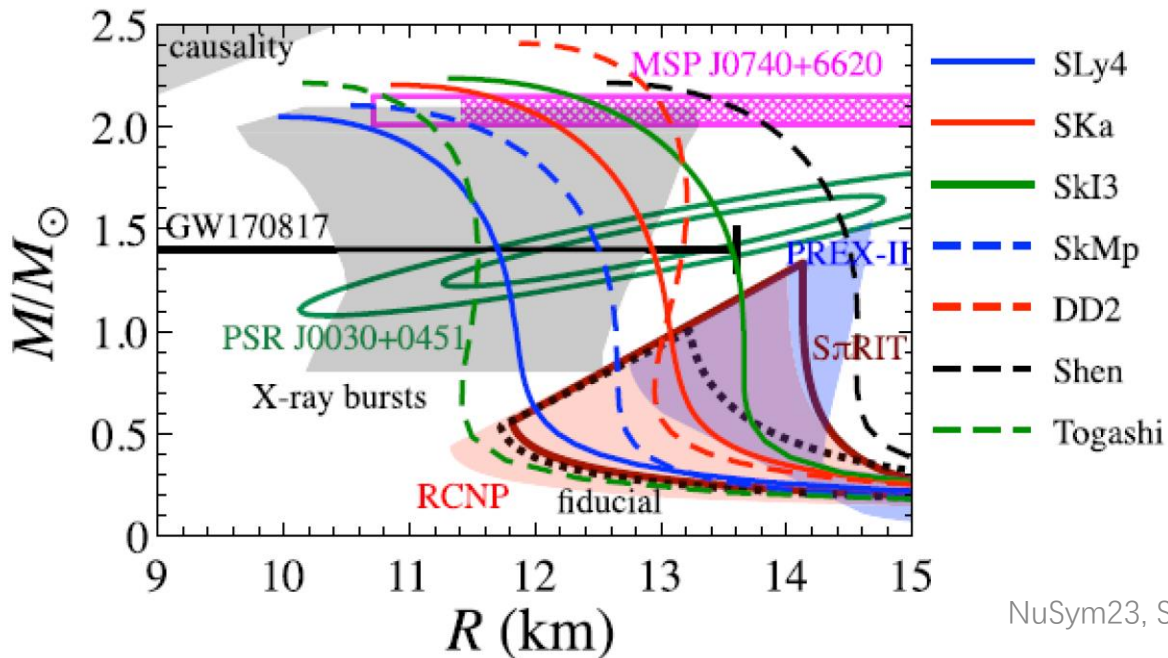
($\rho \sim \rho_0$)

Liquid drop model: $E_{\text{sym}}(\rho_0) \approx 32 \text{ MeV}$

Slope parameter and curvature parameter

$$L \equiv 3\rho_0 \left. \frac{\partial E_{\text{sym}}(\rho)}{\partial \rho} \right|_{\rho=\rho_0} \quad K_{\text{sym}} \equiv 9\rho_0^2 \left. \frac{\partial^2 E_{\text{sym}}(\rho)}{\partial \rho^2} \right|_{\rho=\rho_0}$$

Hajime Sotani, Nobuya Nishimura, and Tomoya Naito,
Prog. Theor. Exp. Phys. 041D01 (2022)

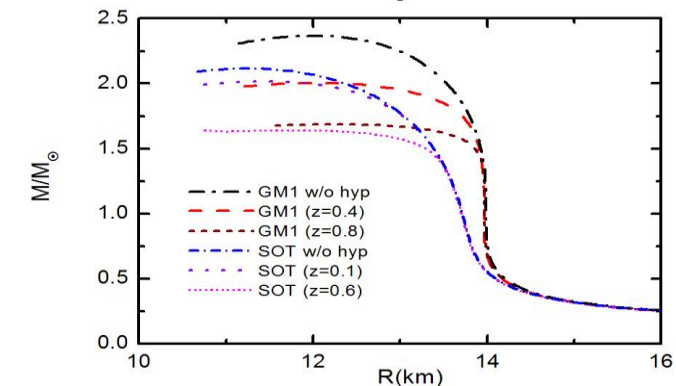
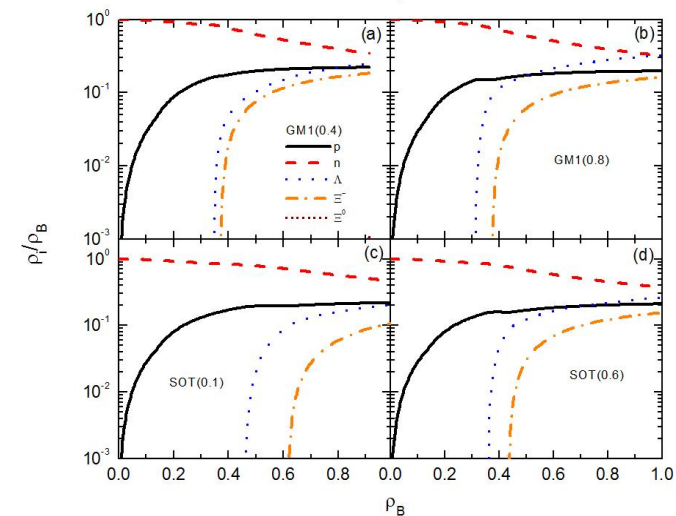
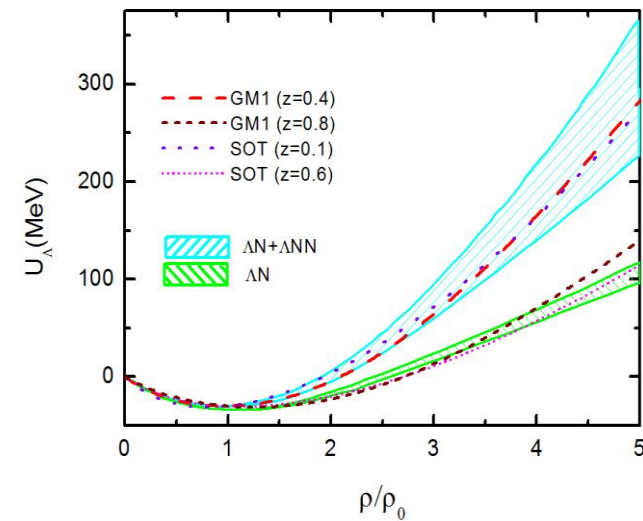
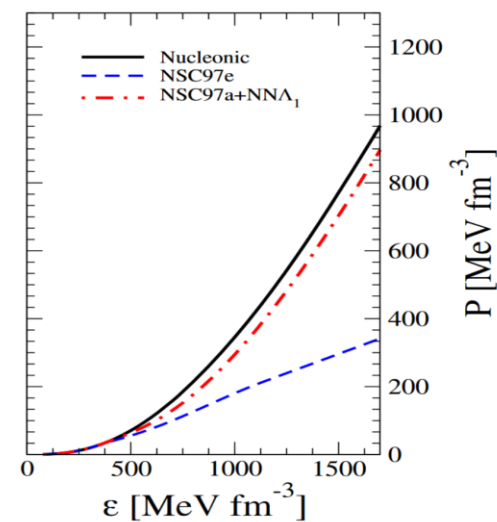
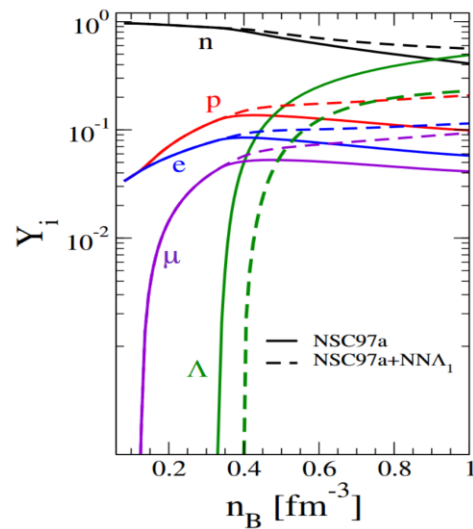
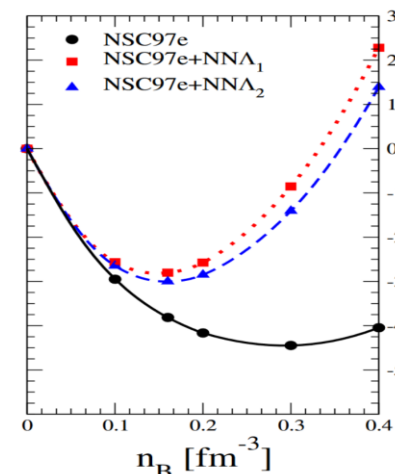
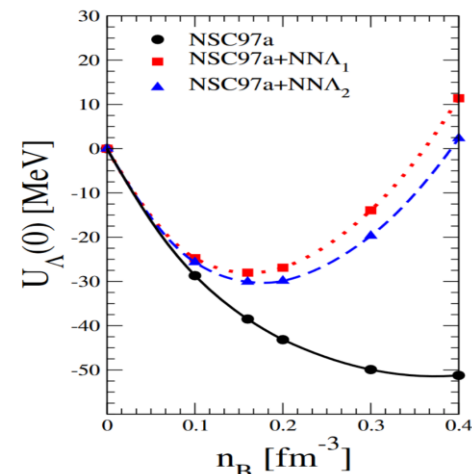
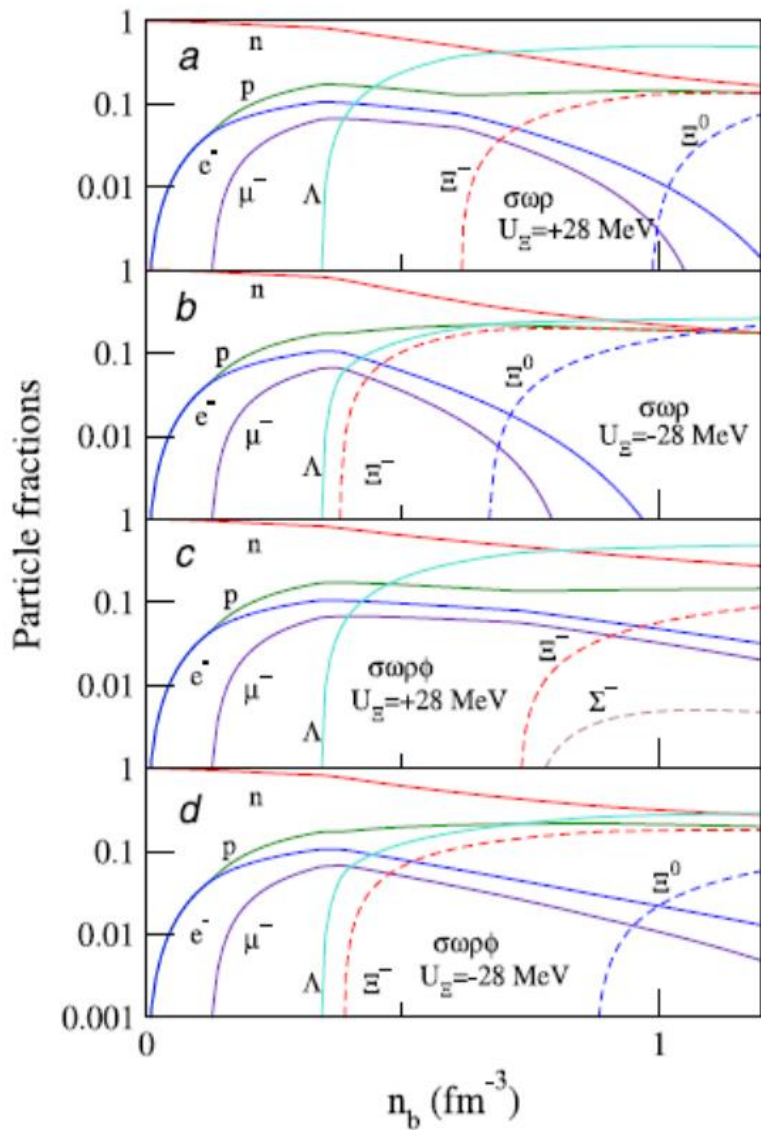


Hyperons in neutron stars

S. Weissenborn, D. Chatterjee, J. Schaffner-Bielich, Nucl. Phys. A 881, 62 (2012)

D. Logoteta, I. Vidaña, I. Bombaci, Eur. Phys. J. A 55, 207 (2019)

S. N. Wei, Z. Q. Feng, in preparation



Transport models for heavy-ion collisions

Progress in Particle and Nuclear Physics 125 (2022) 103962

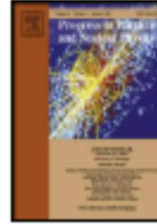


ELSEVIER

Contents lists available at ScienceDirect

Progress in Particle and Nuclear Physics

journal homepage: www.elsevier.com/locate/ppnp



Review

Transport model comparison studies of intermediate-energy heavy-ion collisions

Hermann Wolter^{1,*}, Maria Colonna², Dan Cozma³, Pawel Danielewicz^{4,5}, Che Ming Ko⁶, Rohit Kumar⁴, Akira Ono⁷, ManYee Betty Tsang^{4,5}, Jun Xu^{8,9}, Ying-Xun Zhang^{10,11}, Elena Bratkovskaya^{12,13}, Zhao-Qing Feng¹⁴, Theodoros Gaitanos¹⁵, Arnaud Le Fèvre¹², Natsumi Ikeno¹⁶, Youngman Kim¹⁷, Swagata Mallik¹⁸, Paolo Napolitani¹⁹, Dmytro Oliinychenko²⁰, Tatsuhiko Ogawa²¹, Massimo Papa², Jun Su²², Rui Wang^{9,23}, Yong-Jia Wang²⁴, Janus Weil²⁵, Feng-Shou Zhang^{26,27}, Guo-Qiang Zhang⁹, Zhen Zhang²², Joerg Aichelin²⁸, Wolfgang Cassing²⁵, Lie-Wen Chen²⁹, Hui-Gan Cheng¹⁴, Hannah Elfner^{12,13,20}, K. Gallmeister²⁵, Christoph Hartnack²⁸, Shintaro Hashimoto²¹, Sangyong Jeon³⁰, Kyungil Kim¹⁷, Myungkuk Kim³¹, Bao-An Li³², Chang-Hwan Lee³³, Qing-Feng Li^{24,34}, Zhu-Xia Li¹⁰, Ulrich Mosel²⁵, Yasushi Nara³⁵, Koji Niita³⁶, Akira Ohnishi³⁷, Tatsuhiko Sato²¹, Taesoo Song¹², Agnieszka Sorensen^{38,39}, Ning Wang^{11,40}, Wen-Jie Xie⁴¹, (TMEP collaboration)

Table 1

List of transport models that participated in the TMEP code comparisons discussed in this paper. The columns give the information on the name of the code, the main correspondents of the code, the energy range intended for the code, the treatment of effects of relativity (see Section 2.1), and the comparisons in which the code participated. The different comparisons are listed in the last column in the table by a numbers n , which refer to the subsections 3.n, where they are described in detail: $n = 1$ for Au+Au collisions around 1 AGeV, $n = 2$ for Au+Au collision at 100 and 400 AMeV, $n = 3$ for box-Vlasov, $n = 4$ for box-cascade with only nucleons, $n = 5$ for box-cascade with pion and Δ resonance production, and $n = 6$ for the prediction of pion ratios for Sn+Sn collisions.

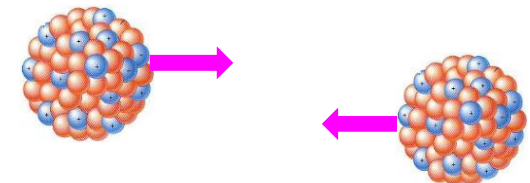
BUU Type	Code Correspondents	Energy Range [A GeV]	Relativity	Comparisons
BLOB	P. Napolitani, M. Colonna	0.01–0.5	non-rel	2
BUU-VM	S. Mallik	0.02–1	rel	3,4,5
DJBUU	Y. Kim, S. Jeon, M. Kim, C.-H. Lee, K. Kim	0.05–2	cov	3
GiBUU	J. Weil, T. Gaitanos, K. Gallmeister, U. Mosel	0.05–40	rel/cov	1,2,3,4
IBL	W.J. Xie, F.S. Zhang	0.05–2	rel	2
IBUU	J. Xu, L.W. Chen, B.A. Li	0.05–2	rel	2,3,4,5
LBUU(LHV)	R. Wang, Z. Zhang, L.-W. Chen	0.01–1.5	rel	3
pBUU	P. Danielewicz	0.01–12	rel	1,2,3,4,5,6
PHSD	E. Bratkovskaya, W. Cassing	0.1–200	rel/cov	1,6
RBUU	T. Gaitanos	0.05–2	cov	1,2
RVUU	Z. Zhang, C.M. Ko, T. Song	0.05–2	cov	1,2,3,4,5
SMASH	D. Oliinychenko, H. Elfner, A. Sorensen	0.5–200	cov	3,4,5,6
SMF	M. Colonna, P. Napolitani	0.01–0.5	non-rel	2,3,4
χ BUU	Z. Zhang, C.M. Ko	0.01–0.5	non-rel	6

QMD Type	Code Correspondents	Energy Range [AGeV]	Relativity	Comparisons
AMD	A. Ono	0.01–0.3	non-rel	2
AMD+JAM	N. Ikeno, A. Ono	0.01–0.3	non-rel+rel	6
BQMD/IQMD	A. Le Fèvre, J. Aichelin, C. Hartnack, R. Kumar	0.05–2	rel	1,2,6
CoMD	M. Papa	0.01–0.3	non-rel	2,4
ImQMD	Y.X. Zhang, N. Wang, Z.X. Li	0.02–0.4	rel	2,3,4
IQMD-BNU	J. Su, F.S. Zhang	0.05–2	rel	2,3,4,5,6
IQMD-SINAP	G.Q. Zhang	0.05–2	rel	2
JAM	A. Ono, N. Ikeno, Y. Nara, A. Ohnishi	1–158	rel	4,5
JQMD 2.0	T. Ogawa, K. Niita, S. Hashimoto, T. Sato	0.01–3	rel	4,5
LQMD(IQMD-IMP)	Z.Q. Feng, H.G. Cheng	0.01–10	rel	2,3,4,5
TuQMD/dcQMD	D. Cozma	0.1–2	rel	1,2,3,4,5,6
UrQMD	Y. J. Wang, Q. F. Li, Y. X. Zhang	0.05–200	rel	1,2,3,4,6

II. Transport approach for NS matter properties (LQMD)

Heavy-ion collisions (5 MeV – 5 GeV/nucleon) and hadron induced reaction (p , \bar{p} , π , K , e , etc)

- **Lanzhou quantum molecular dynamics** (Skyrme interaction, Walecka model with σ , ω , ρ , δ)
- **Isospin physics at intermediate energies** (constraining nuclear **symmetry energy** at sub- and supra-saturation densities in HICs and probing isospin splitting of nucleon effective mass from HICs)
- **In-medium properties of hadrons in dense nuclear matter from heavy-ion collisions** (extracting optical potentials, i.e., $\Delta(1232)$, $N^*(1440)$, $N^*(1535)$), hyperons (Λ, Σ, Ξ) and mesons ($\pi, K, \eta, \rho, \omega, \phi \dots$), hypernucleus dynamics)
- **Nuclear cluster and hypernuclear cluster production** (production cross section, transverse momentum spectra, rapidity distribution, collective flows, e.g., $\Lambda(\Sigma)X$, $\Lambda\Lambda X$, ΞX , $\bar{\Lambda}X(S=1)$)
- **Hadron induced nuclear reactions** (physics at PANDA such as hypernuclear, neutron skin thickness etc)



1. Skyrme energy-density functional (LQMD-Skyrme)

PHYSICAL REVIEW C 84, 024610 (2011)

Momentum dependence of the symmetry potential and its influence on nuclear reactions

Zhao-Qing Feng*

Institute of Modern Physics, Chinese Academy of Sciences, Lanzhou 730000, People's Republic of China

(Received 11 July 2011; published 19 August 2011)

$$H_B = \sum_i \sqrt{\mathbf{p}_i^2 + \mathbf{m}_i^2} + U_{\text{int}} + U_{\text{mom}}$$

$$U_{\text{loc}} = \int V_{\text{loc}}(\rho(\mathbf{r})) d\mathbf{r}$$

$$V_{\text{loc}}(\rho) = \frac{\alpha}{2} \frac{\rho^2}{\rho_0} + \frac{\beta}{1+\gamma} \frac{\rho^{1+\gamma}}{\rho_0^\gamma} + E_{\text{sym}}^{\text{loc}}(\rho) \rho \delta^2 + \frac{g_{\text{sur}}}{2\rho_0} (\nabla \rho)^2 + \frac{g_{\text{sur}}^{\text{iso}}}{2\rho_0} [\nabla(\rho_n - \rho_p)]^2,$$

$$U_{\text{mom}} = \frac{1}{2\rho_0} \sum_{i,j,j \neq i} \sum_{\tau,\tau'} C_{\tau,\tau'} \delta_{\tau,\tau_i} \delta_{\tau',\tau_j} \iiint d\mathbf{p} d\mathbf{p}' d\mathbf{r} f_i(\mathbf{r}, \mathbf{p}, t) \times [\ln(\epsilon(\mathbf{p} - \mathbf{p}')^2 + 1)]^2 f_j(\mathbf{r}, \mathbf{p}', t).$$

$$E_{\text{sym}}(\rho) = \frac{1}{3} \frac{\hbar^2}{2m} \left(\frac{3}{2} \pi^2 \rho \right)^{2/3} + E_{\text{sym}}^{\text{loc}}(\rho) + E_{\text{sym}}^{\text{mom}}(\rho).$$

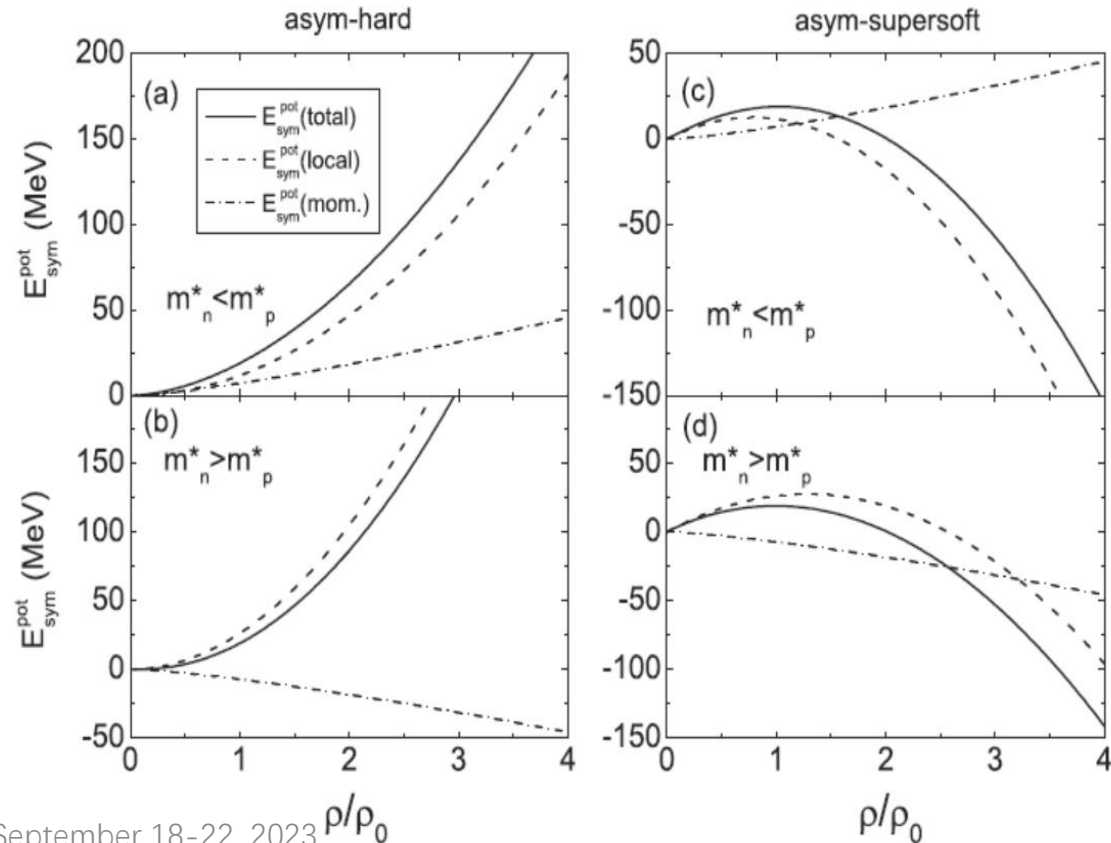
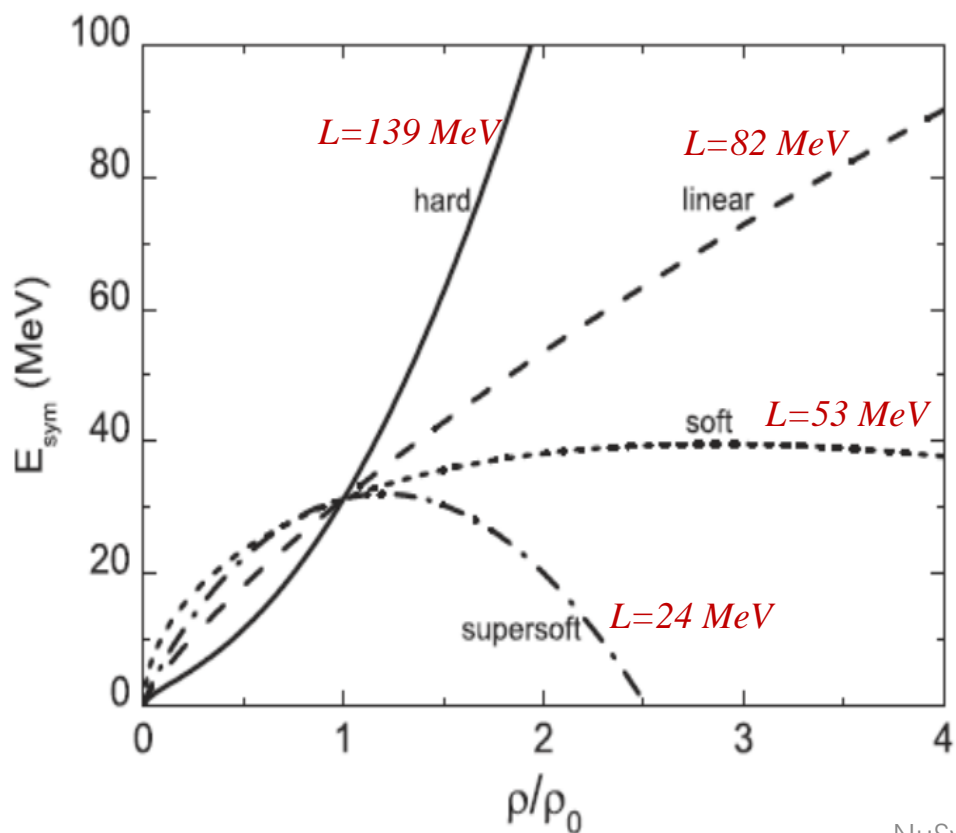
$$E_{\text{sym}}^{\text{loc}}(\rho) = \frac{1}{2} C_{\text{sym}} (\rho/\rho_0)^{\gamma_s}$$

$$E_{\text{sym}}^{\text{loc}}(\rho) = a_{\text{sym}} (\rho/\rho_0) + b_{\text{sym}} (\rho/\rho_0)^2.$$

$$\begin{aligned} C_{\text{sym}} &= 38 \text{ MeV} \\ a_{\text{sym}} &= 37.7 \text{ MeV} \\ b_{\text{sym}} &= -18.7 \text{ MeV} \end{aligned}$$

Table 1: The parameters and properties of isospin symmetric EoS used in the LQMD model at the density of 0.16 fm^{-3} .

Parameters	α (MeV)	β (MeV)	γ	C_{mom} (MeV)	ϵ (c^2/MeV^2)	m_∞^*/m	K_∞ (MeV)
PAR1	-215.7	142.4	1.322	1.76	5×10^{-4}	0.75	230
PAR2	-226.5	173.7	1.309	0.	0.	1.	230



2. Covariant energy-density functional (LQMD-RMF)

Si-Na Wei, Zhao-Qing Feng, arXiv:2302.09984

$$L = \bar{\psi} [i\gamma_\mu \partial^\mu - (M_N - g_\sigma \varphi - g_\delta \vec{\tau} \cdot \vec{\delta}) - g_\omega \gamma_\mu \omega^\mu - g_\rho \gamma_\mu \vec{\tau} \cdot \vec{b}^\mu] \psi \\ + \frac{1}{2} (\partial_\mu \varphi \partial^\mu \varphi - m_\sigma^2 \varphi^2) - U(\varphi) + \frac{1}{2} (\partial_\mu \vec{\delta} \partial^\mu \vec{\delta} - m_\delta^2 \vec{\delta}^2) \\ + \frac{1}{2} m_\omega^2 \omega_\mu \omega^\mu - \frac{1}{4} F_{\mu\nu} F^{\mu\nu} + \frac{1}{2} m_\rho^2 \vec{b}_\mu \vec{b}^\mu - \frac{1}{4} \vec{G}_{\mu\nu} \vec{G}^{\mu\nu}$$

$$F_{\mu\nu} = \partial_\mu \omega_\nu - \partial_\nu \omega_\mu, \\ G_{\mu\nu} = \partial_\mu \vec{b}_\nu - \partial_\nu \vec{b}_\mu, \\ U(\varphi) = \frac{g_2}{3} \varphi^3 + \frac{g_3}{4} \varphi^4$$

Energy density functional

$$\varepsilon = \sum_{i=n,p} 2 \int \frac{d^3k}{(2\pi)^3} \sqrt{k^2 + M_i^{*2}} + \frac{1}{2} m_\sigma^2 \varphi^2 + U(\varphi) + \frac{1}{2} m_\omega^2 \omega_0^2 + \frac{1}{2} m_\rho^2 b_0^2 + \frac{1}{2} m_\delta^2 \delta_3^2$$

Temporal evolution in phase space

$$\dot{\mathbf{x}} = \frac{\mathbf{p}_i^*}{p_0^*} + \sum_{i \neq j}^N \left\{ \frac{g_v^2}{2m_v^2} z_j^{*\mu} u_{i,\mu} B_i B_j \frac{\partial \rho_{ij}}{\partial \mathbf{p}_i} + \frac{g_v^2}{2m_v^2} z_i^{*\mu} u_{j,\mu} B_i B_j \frac{\partial \rho_{ji}}{\partial \mathbf{p}_i} + \frac{g_v^2}{2m_v^2} z_j^{*\mu} \rho_{ji} B_i B_j \frac{\partial u_{i,\mu}}{\partial \mathbf{p}_i} \right. \\ \left. + z_j^{*\mu} \frac{B_i B_j \bar{g}_v^2}{2m_v^2} \left[\frac{\rho_{ij}}{1 - p_{T,ij}^2/\Lambda_v^2} \frac{\partial u_{i,\mu}}{\partial \mathbf{p}_i} + \frac{u_{i,\mu}}{1 - p_{T,ij}^2/\Lambda_v^2} \frac{\partial \rho_{ij}}{\partial \mathbf{p}_i} + u_{i,\mu} \rho_{ij} \frac{\partial [1/(1 - p_{T,ij}^2/\Lambda_v^2)]}{\partial \mathbf{p}_i} \right] \right. \\ \left. + z_i^{*\mu} \frac{B_i B_j \bar{g}_v^2}{2m_v^2} \left[\frac{u_{j,\mu}}{1 - p_{T,ji}^2/\Lambda_v^2} \frac{\partial \rho_{ji}}{\partial \mathbf{p}_i} + u_{j,\mu} \rho_{ji} \frac{\partial [1/(1 - p_{T,ji}^2/\Lambda_v^2)]}{\partial \mathbf{p}_i} \right] \right. \\ \left. - \frac{m_j^*}{p_j^{*0}} \frac{\partial S_j}{\partial \mathbf{p}_i} - \frac{m_i^*}{p_i^{*0}} \frac{\partial S_i}{\partial \mathbf{p}_i} \right\},$$

$$\dot{\mathbf{p}} = - \sum_{i \neq j}^N \left\{ \frac{g_v^2}{2m_v^2} z_j^{*\mu} u_{i,\mu} B_i B_j \frac{\partial \rho_{ij}}{\partial \mathbf{r}_i} + \frac{g_v^2}{2m_v^2} z_i^{*\mu} u_{j,\mu} B_i B_j \frac{\partial \rho_{ji}}{\partial \mathbf{r}_i} \right. \\ \left. + z_j^{*\mu} \frac{B_i B_j \bar{g}_v^2}{2m_v^2} \frac{u_{i,\mu}}{1 - p_{T,ij}^2/\Lambda_v^2} \frac{\partial \rho_{ij}}{\partial \mathbf{r}_i} \right. \\ \left. + z_i^{*\mu} \frac{B_i B_j \bar{g}_v^2}{2m_v^2} \frac{u_{j,\mu}}{1 - p_{T,ji}^2/\Lambda_v^2} \frac{\partial \rho_{ji}}{\partial \mathbf{r}_i} \right. \\ \left. - \frac{m_j^*}{p_j^{*0}} \frac{\partial S_j}{\partial \mathbf{r}_i} - \frac{m_i^*}{p_i^{*0}} \frac{\partial S_i}{\partial \mathbf{r}_i} \right\},$$

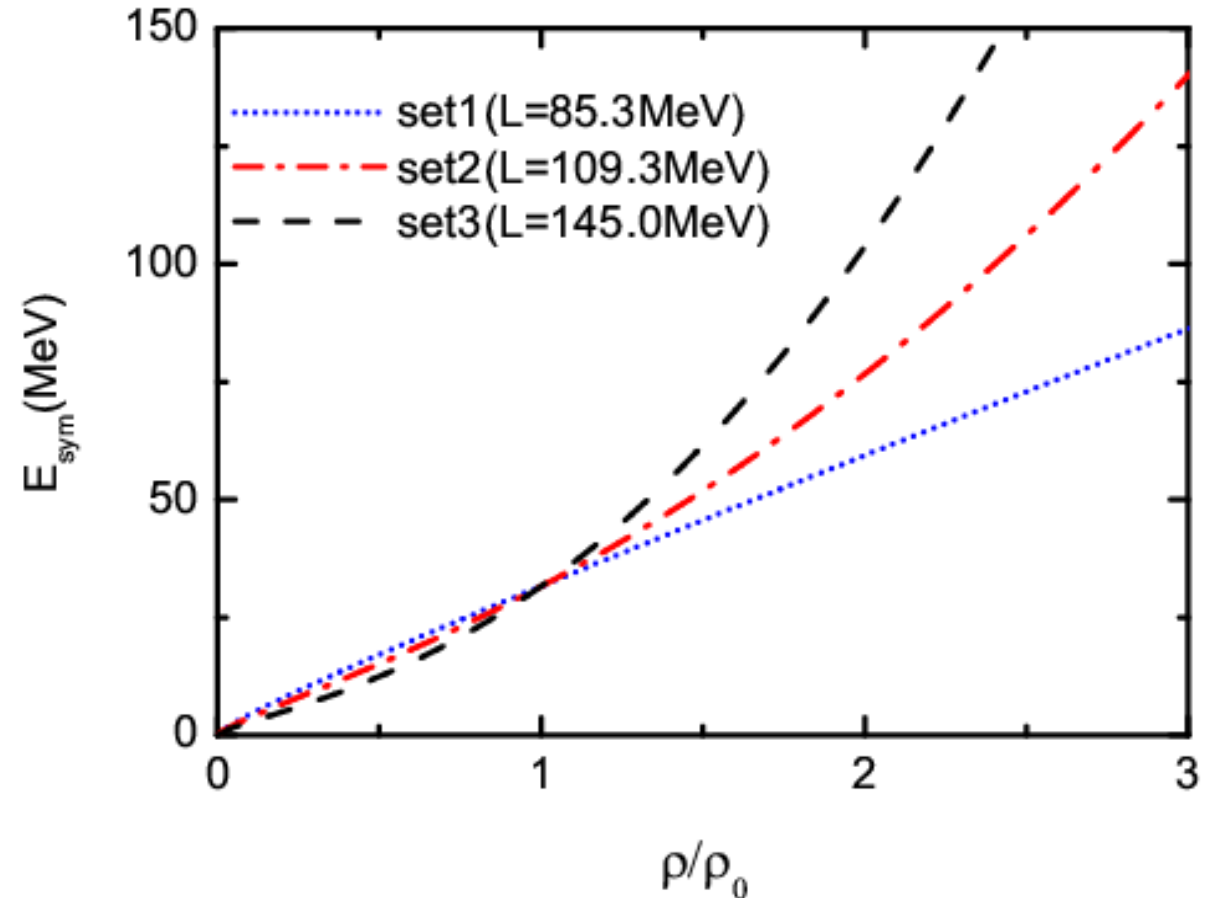
TABLE I: Parameter sets for RMF. The saturation density ρ_0 is set to be 0.16 fm^{-3} . The binding energy of saturation density is $E/A - M_N = -16 \text{ MeV}$. The isoscalar-vector ω and isovector-vector ρ masses are fixed to their physical values, $m_\omega = 783 \text{ MeV}$ and $m_\rho = 763 \text{ MeV}$. The remaining meson mass m_σ is set to be 550 MeV .

model	g_σ	g_ω	$g_2 \text{ (fm}^{-1}\text{)}$	g_3	g_ρ	g_δ	$K \text{ (MeV)}$	$E_{sym}(\rho_0) \text{ (MeV)}$	$L(\rho_0) \text{ (MeV)}$
set1	8.145	7.570	31.820	28.100	4.049	-	230	31.6	85.3
set2	8.145	7.570	31.820	28.100	8.673	5.347	230	31.6	109.3
set3	8.145	7.570	31.820	28.100	11.768	7.752	230	31.6	145.0

Symmetry energy in LQMD-RMF

$$E_{sym} = \frac{1}{6} \frac{k_F^2}{E_F^*} + \frac{1}{2} \left[f_\rho - f_\delta \left(\frac{M^*}{E_F^*} \right) \right] \rho$$

$$f_{\rho,\delta} = g_{\rho,\delta} / m_{\rho,\delta}$$



3. hadron-hadron scattering channels

π and resonances ($\Delta(1232)$, $N^*(1440)$, $N^*(1535)$, ...) production:

$$\begin{aligned}
 NN &\leftrightarrow N\Delta, & NN &\leftrightarrow NN^*, & NN &\leftrightarrow \Delta\Delta, & \Delta &\leftrightarrow N\pi, \\
 N^* &\leftrightarrow N\pi, & NN &\leftrightarrow NN\pi(s\text{-state}), & N^*(1535) &\leftrightarrow N\eta
 \end{aligned}$$

Collisions between resonances, $NN^* \leftrightarrow N\Delta$, $NN^* \leftrightarrow NN^*$

Strangeness channels:

$$\begin{aligned}
 BB &\rightarrow BYK, & BB &\rightarrow BBK\bar{K}, & B\pi(\eta) &\rightarrow YK, & YK &\rightarrow B\pi, \\
 B\pi &\rightarrow NK\bar{K}, & Y\pi &\rightarrow B\bar{K}, & B\bar{K} &\rightarrow Y\pi, & YN &\rightarrow \bar{K}NN, \\
 BB &\rightarrow B\Xi KK, & \bar{K}B &\leftrightarrow K\Xi, & YY &\leftrightarrow N\Xi, & \bar{K}Y &\leftrightarrow \pi\Xi.
 \end{aligned}$$

Reaction channels with antiproton:

$$\bar{p}N \rightarrow \bar{N}N, \quad \bar{N}N \rightarrow \bar{N}N, \quad \bar{N}N \rightarrow \bar{B}B, \quad \bar{N}N \rightarrow \bar{Y}Y$$

$$\bar{N}N \rightarrow \text{annihilation}(\pi, \eta, \rho, \omega, K, \bar{K}, K^*, \bar{K}^*, \phi)$$

Statistical model with SU(3) symmetry for annihilation

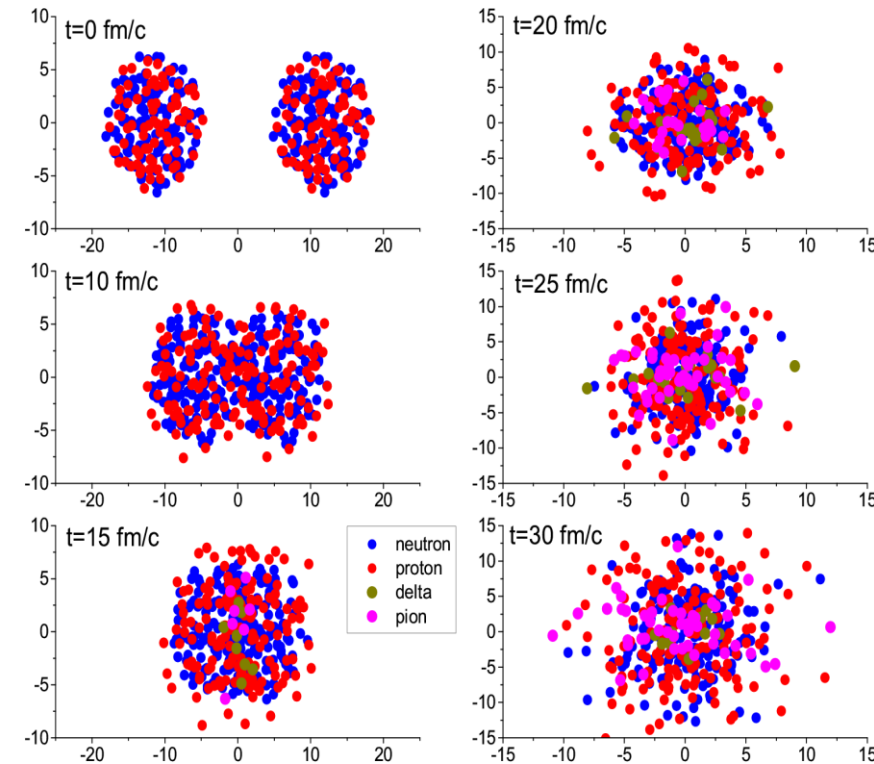
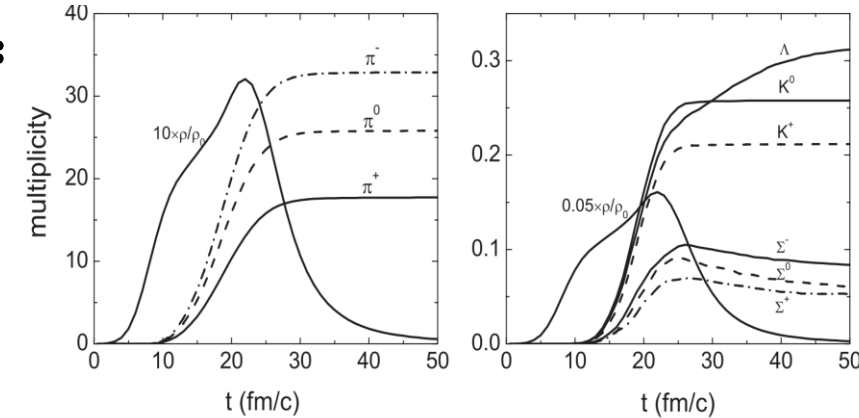
(E.S. Golubeva et al., Nucl. Phys. A 537, 393 (1992))

Dynamics of strangeness production in heavy-ion collisions near threshold energies

Zhao-Qing Feng* and Gen-Ming Jin

Institute of Modern Physics, Chinese Academy of Sciences, Lanzhou 730000, People's Republic of China

(Received 20 September 2010; published 29 November 2010)



4. Pion-nucleon potential

$$\omega_{\tau_z}(\rho, \vec{p}) = \omega_{\text{isoscalar}}(\rho, \vec{p}) + C_{\text{iso}}^{\pi} \tau_z \delta \left(\frac{\rho}{\rho_0} \right)^{\gamma_{\pi}}$$

$$C_{\pi} = \rho_0 \hbar^3 / (4 f_{\pi}^2) = 36 \text{ MeV},$$

$\tau_z = 1, 0, -1$ for π^{-}, π^0 and π^{+}

Evaluation of $\omega_{\text{isoscalar}}$

1) phenomenological ansatz from pionic atom

C. Gale and J. Kapusta, Phys. Rev. C 35, 2107 (1987);

C. Fuchs et al., Phys. Rev. C 55, 411 (1997);

Z. Q. Feng and G. M. Jin, Phys. Rev. C 82, 044615 (2010)

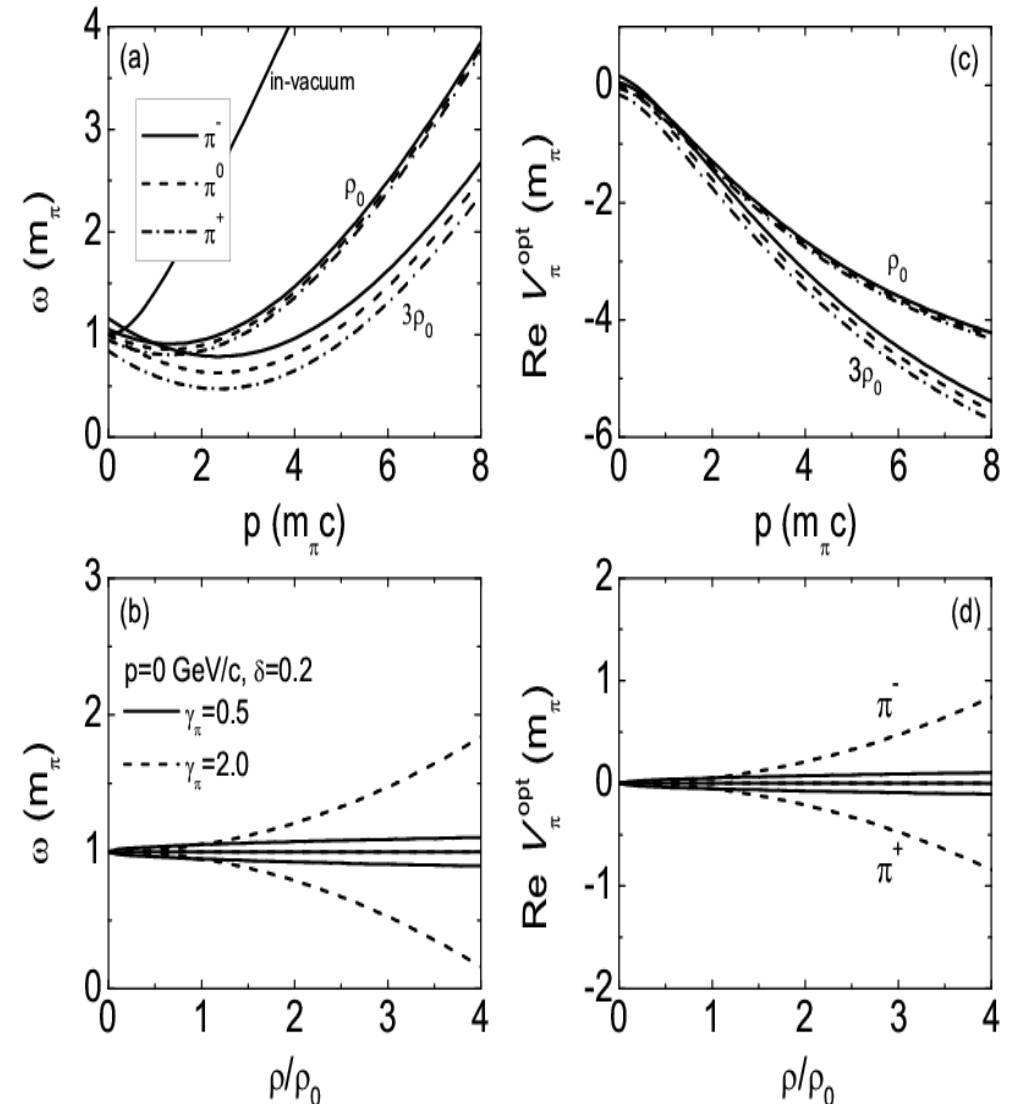
2) Δ -hole model

L. Xiong, C. M. Ko, V. Koch, Phys. Rev. C 47, 788 (1993);

C. Fuchs et al., Phys. Rev. C 55, 411 (1997)

$$\omega_{\text{isoscalar}}(\mathbf{p}_i, \rho_i) = S_{\pi}(\mathbf{p}_i, \rho_i) \omega_{\pi\text{-like}}(\mathbf{p}_i, \rho_i) \\ + S_{\Delta}(\mathbf{p}_i, \rho_i) \omega_{\Delta\text{-like}}(\mathbf{p}_i, \rho_i)$$

Z. Q. Feng et al., Phys. Rev. C 92 (2015) 044604



The energy balance in the decay of resonances and reabsorption of pions in nuclear medium $R \leftrightarrow N\pi$

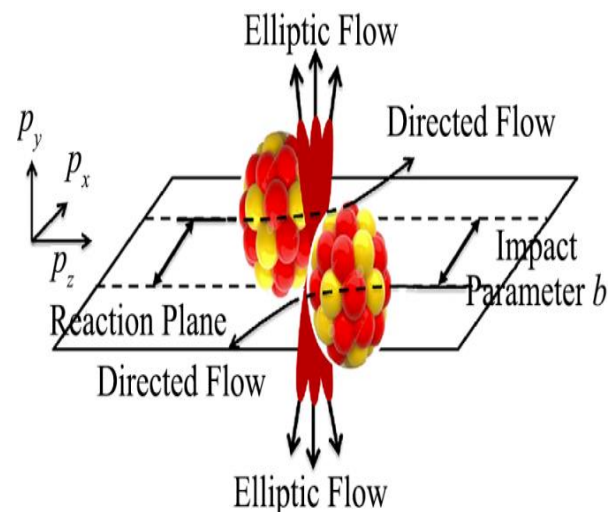
$$\sqrt{m_R^2 + \mathbf{p}_R^2} + U_R(\rho, \delta, \mathbf{p}_R) = \sqrt{m_N^2 + (\mathbf{p}_R - \mathbf{p}_\pi)^2} + U_N(\rho, \delta, \mathbf{p}) + \omega_\pi(\mathbf{p}_\pi, \rho) + V_{\pi N}^{Coul}$$

The resonance production and rescattering in nuclear medium $NN \leftrightarrow NR$ and $NR \leftrightarrow NR'$

$$\sqrt{m_N^2 + \mathbf{p}_1^2} + U_N(\rho, \delta, \mathbf{p}_1) + \sqrt{m_N^2 + \mathbf{p}_2^2} + U_N(\rho, \delta, \mathbf{p}_2) = \sqrt{m_R^2 + \mathbf{p}_R^2} + U_R(\rho, \delta, \mathbf{p}_R) + \sqrt{m_N^2 + \mathbf{p}'^2} + U_N(\rho, \delta, \mathbf{p}')$$

$$U_{\Delta^-} = U_n, \quad U_{\Delta^{++}} = U_p, \quad U_{\Delta^+} = \frac{1}{3}U_n + \frac{2}{3}U_p,$$

$$U_{\Delta^0} = \frac{1}{3}U_p + \frac{2}{3}U_n,$$



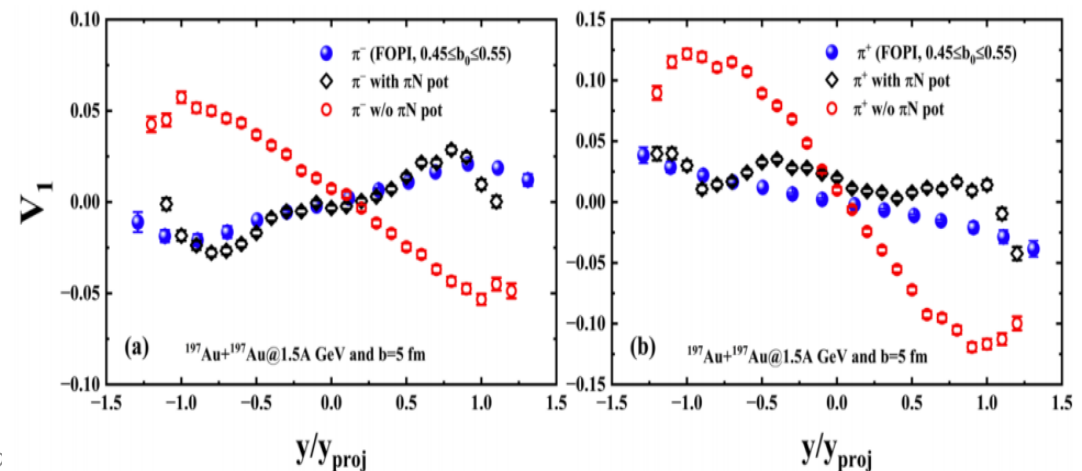
NuSym23, September 18-22

PHYSICAL REVIEW C **108**, 024614 (2023)

Collective flows of clusters and pions in heavy-ion collisions at GeV energies

Heng-Jin Liu, Hui-Gan Cheng, and Zhao-Qing Feng*

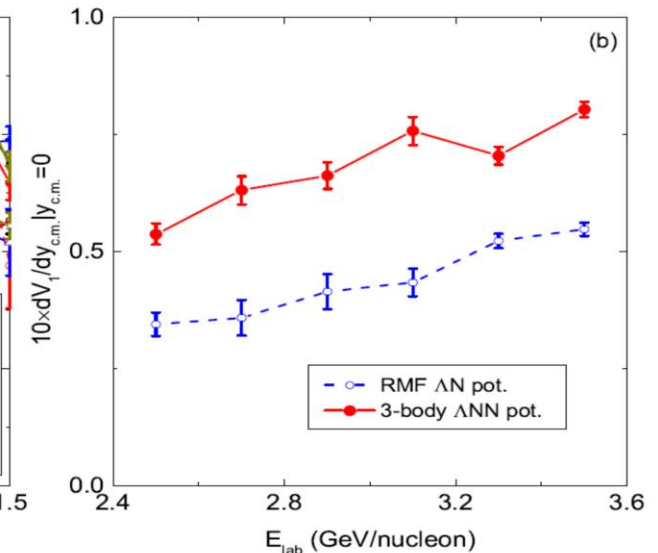
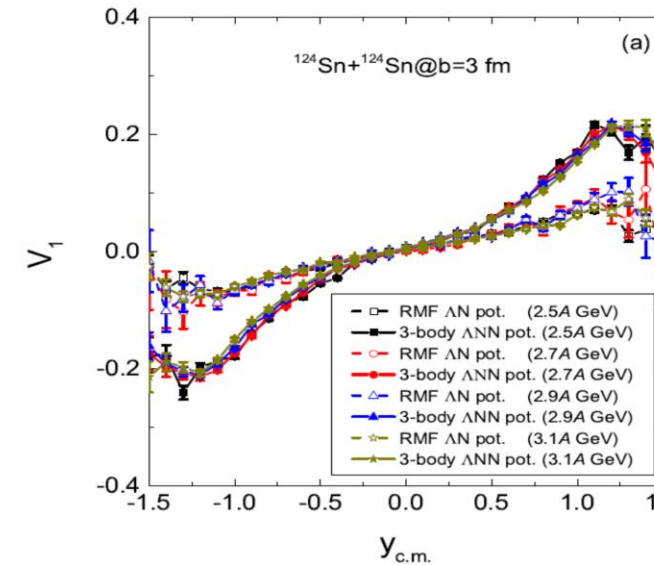
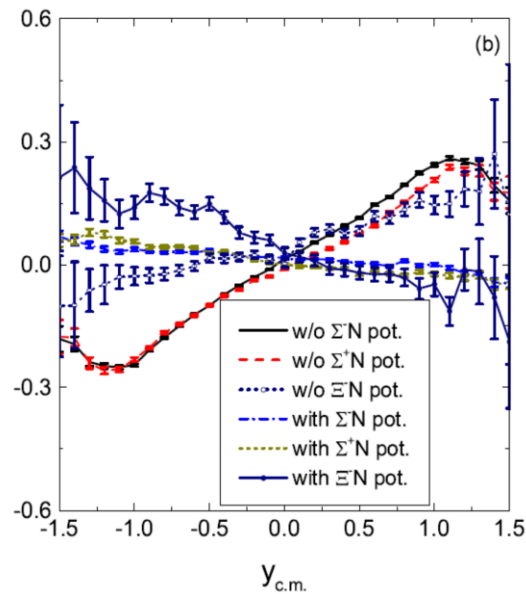
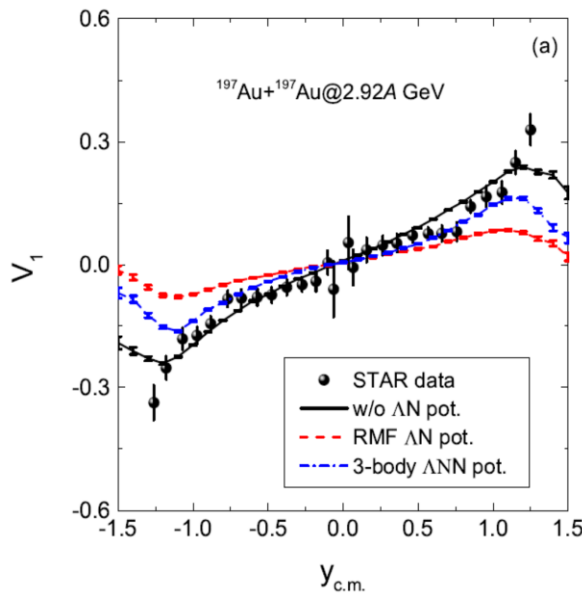
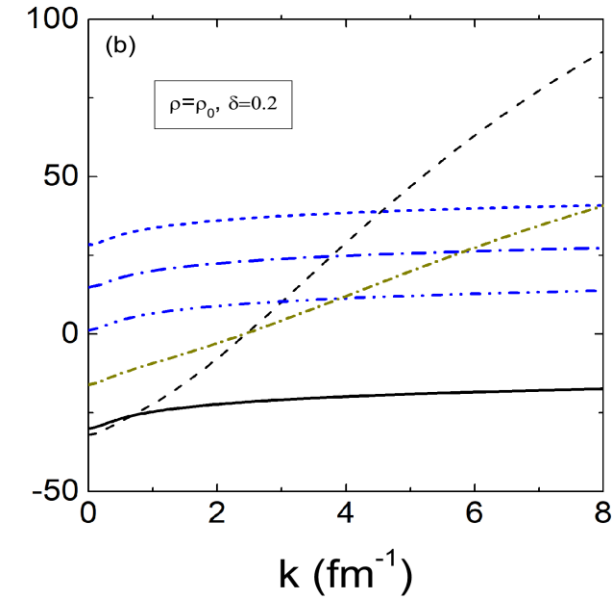
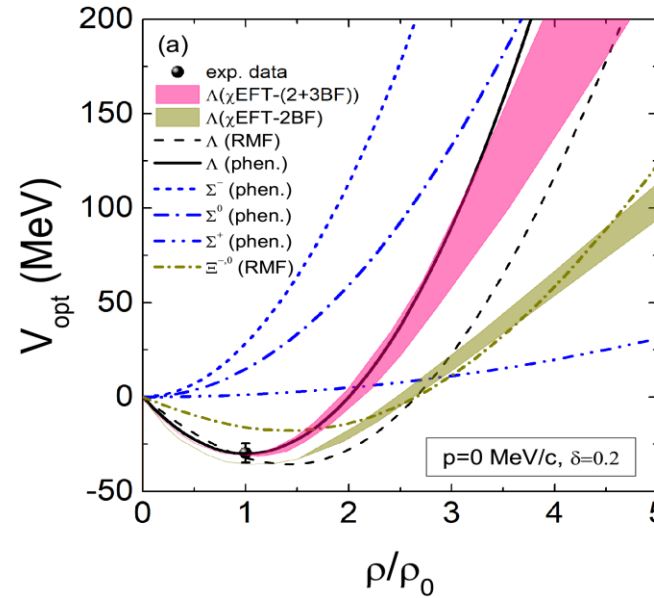
School of Physics and Optoelectronics, South China University of Technology, Guangzhou 510640, China



5. hyperon-nucleon interaction in dense nuclear matter

$$V_{opt}^{\Lambda NN}(\mathbf{p}_i, \rho_i) = V_a(\rho_i/\rho_0) + V_b(\rho_i/\rho_0)^2 + C_{mom} \ln(\epsilon \mathbf{p}_i^2 + 1)$$

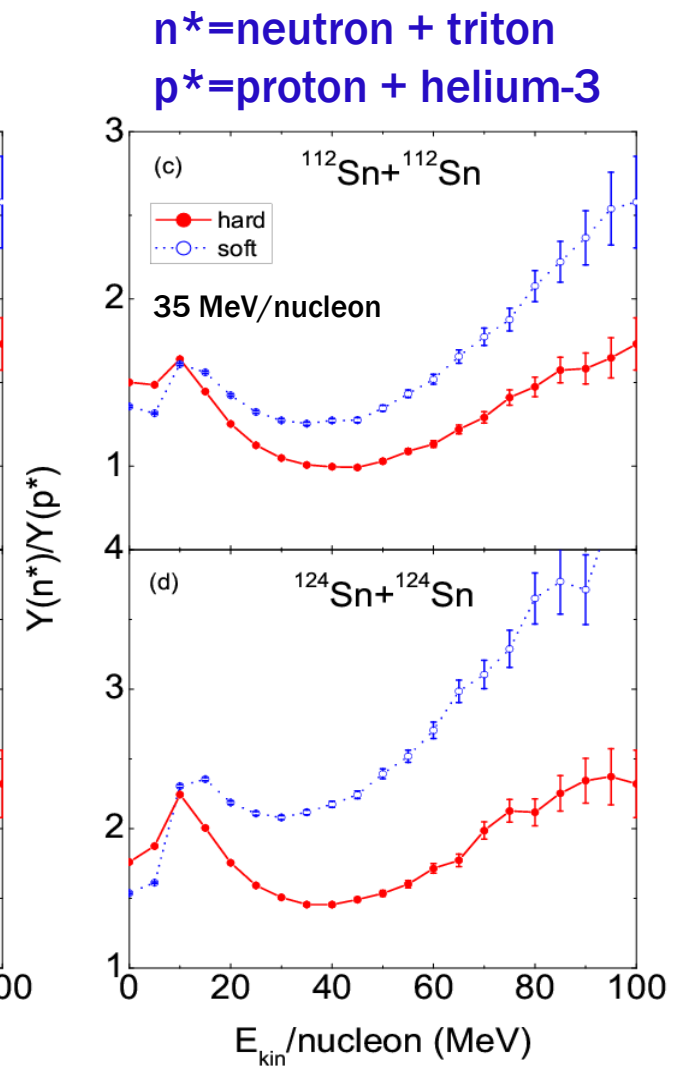
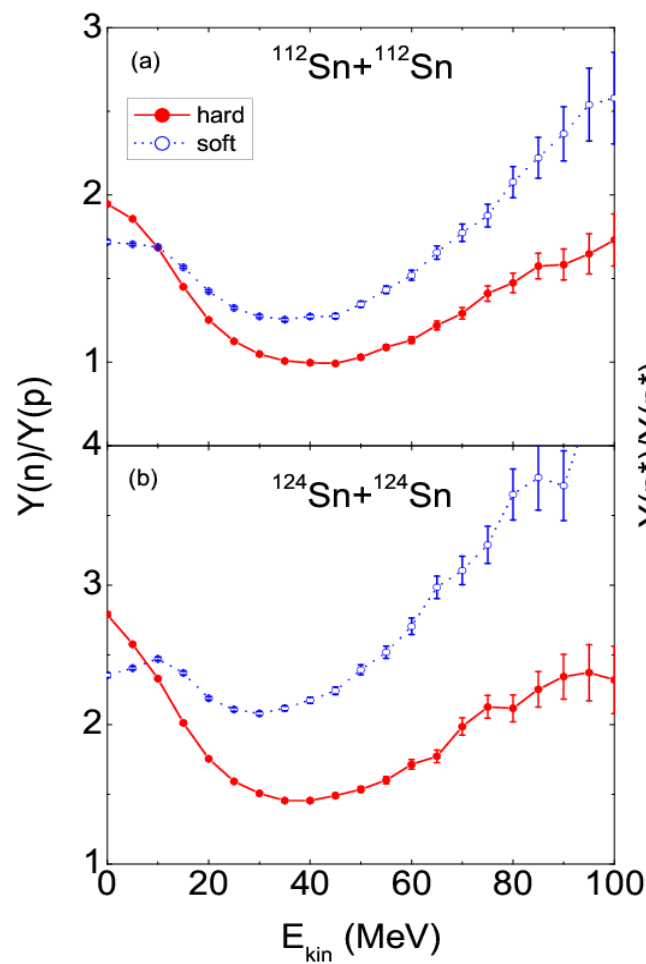
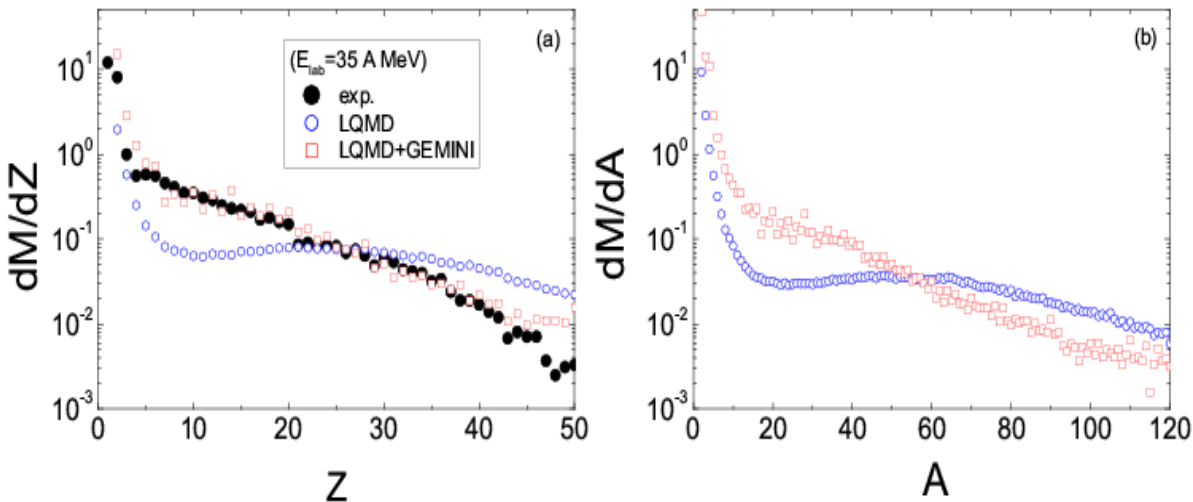
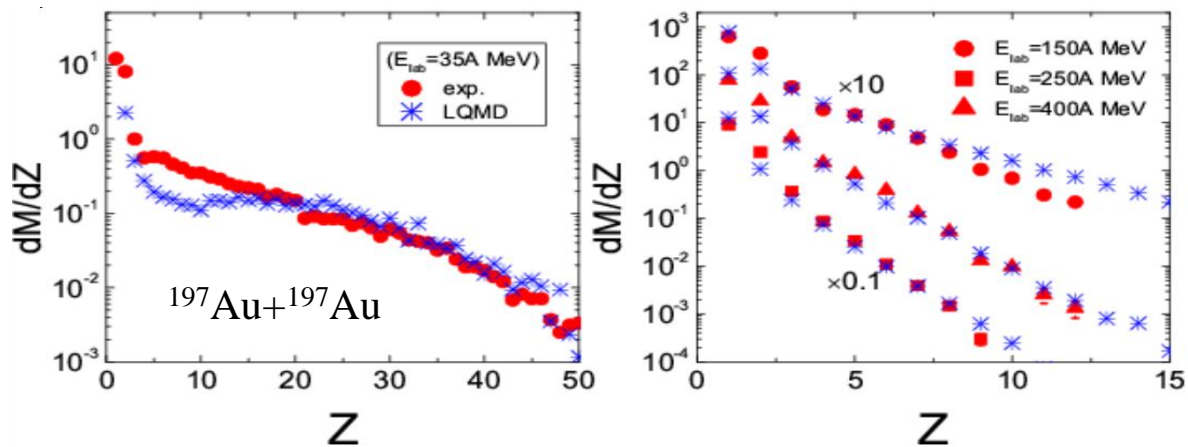
$$V_{opt}^{\Sigma}(\mathbf{p}_i, \rho_i) = V_0(\rho_i/\rho_0)^{\gamma_s} + V_1(\rho_n - \rho_p)t_{\Sigma} \rho_i^{\gamma_s - 1} / \rho_0^{\gamma_s} + C_{mom} \ln(\epsilon \mathbf{p}_i^2 + 1).$$



III. Neutron-star matter properties from HICs

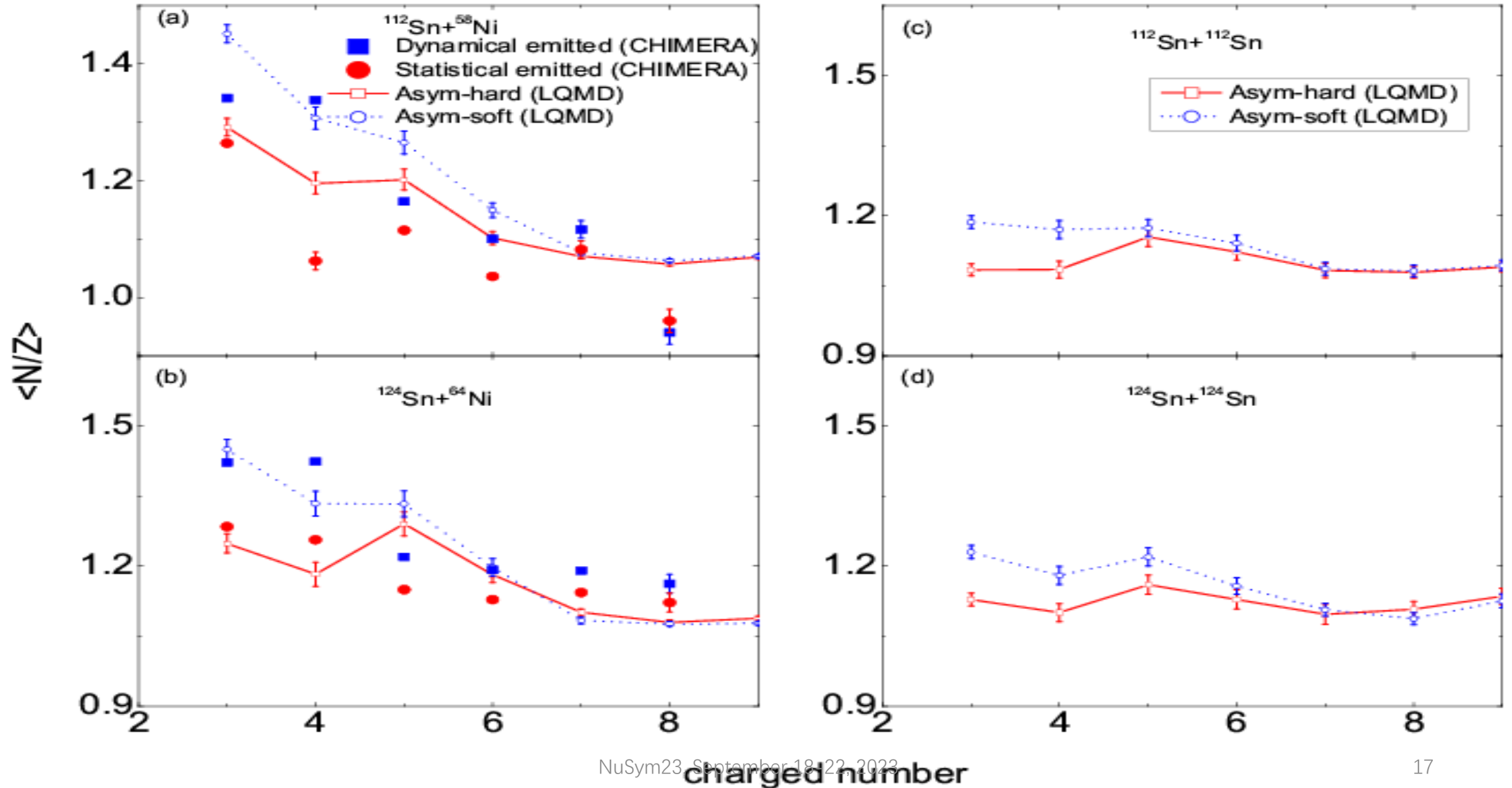
1. Fragmentation reactions and symmetry energy in the sub-saturation density region

Zhao-Qing Feng, Phys. Rev. C 82, 044615 (2010); 94, 014609 (2016))

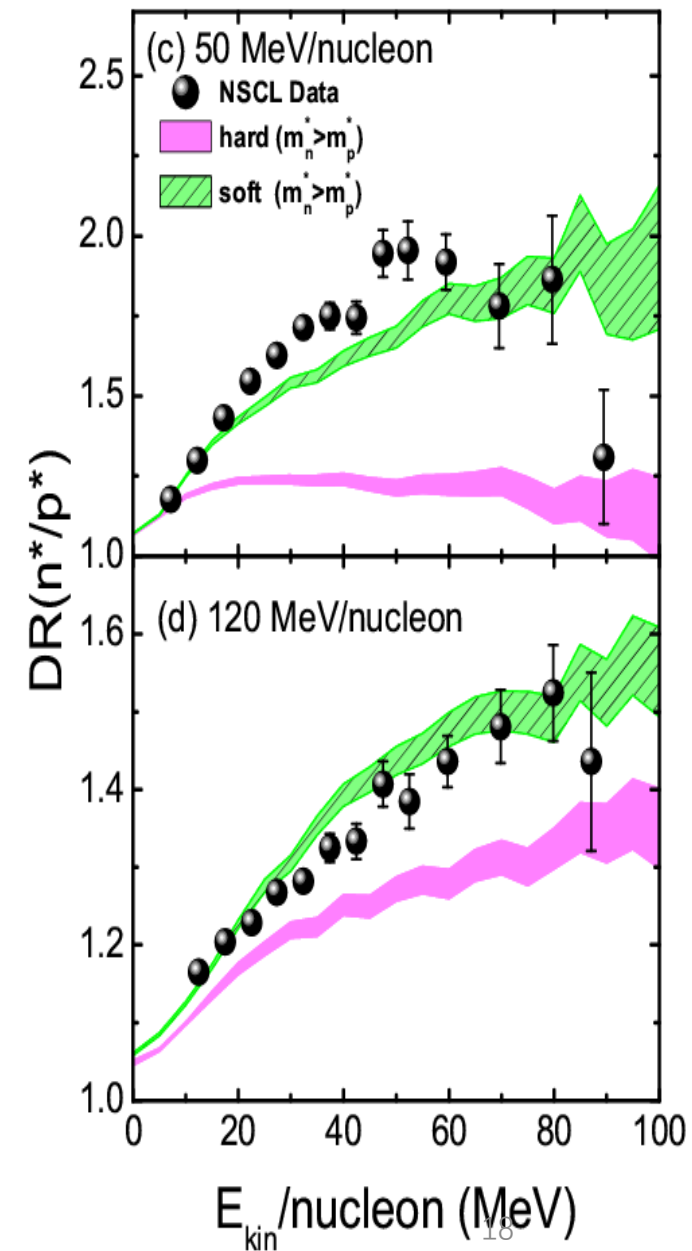
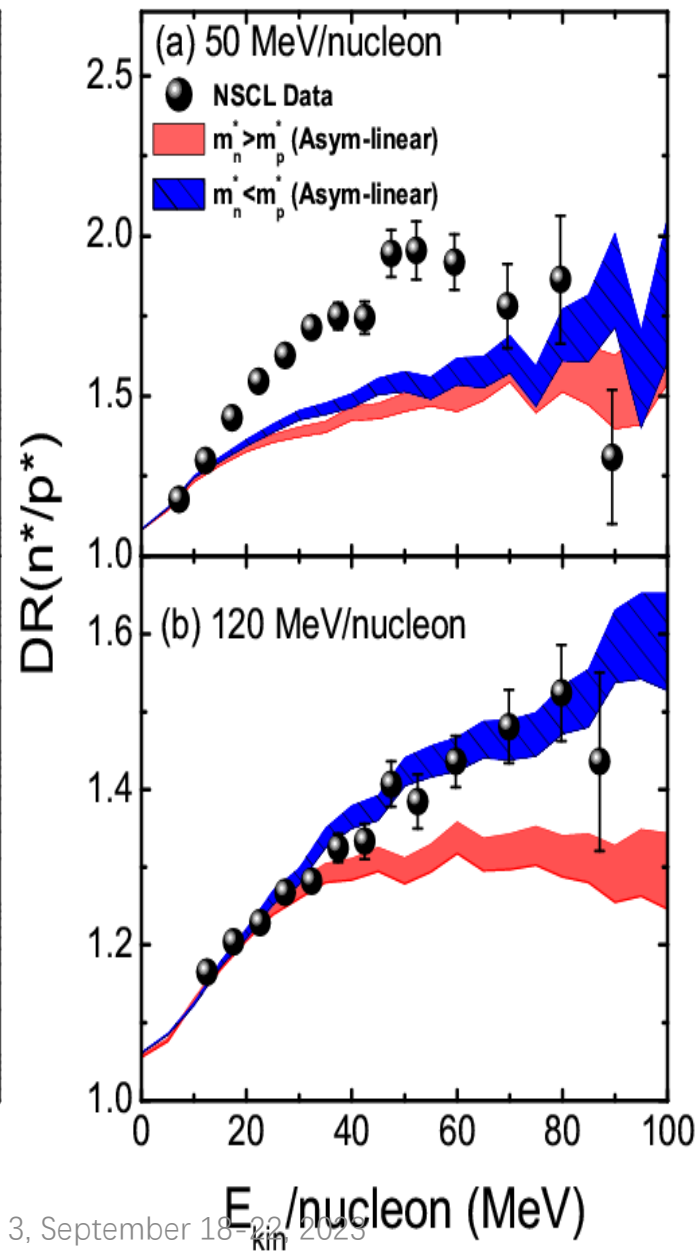
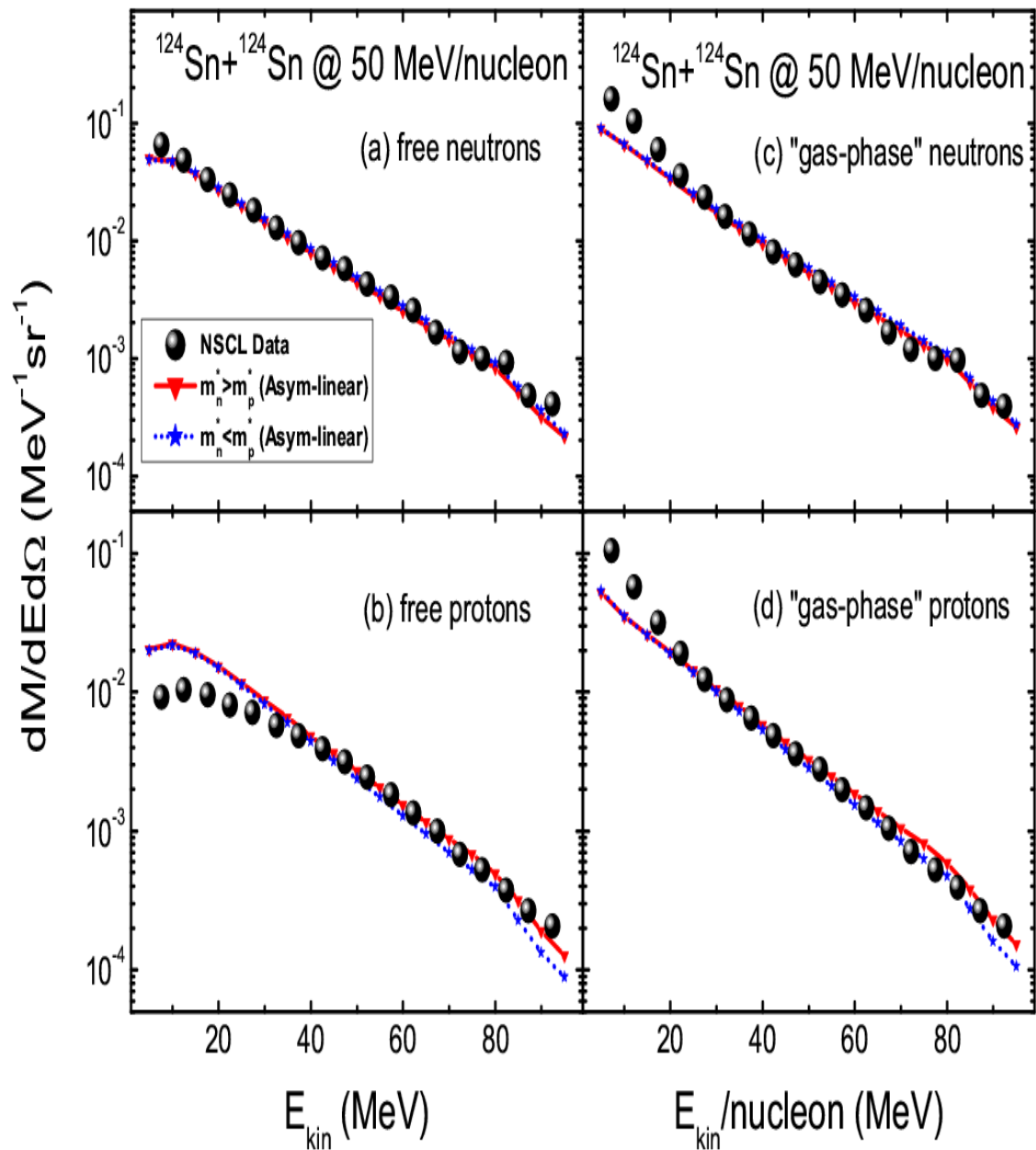


The average neutron to proton ratio of IMFs in isotopic nuclear reactions

Zhao-Qing Feng, PRC 94, 014609 (2016), arXiv: 1603.07138

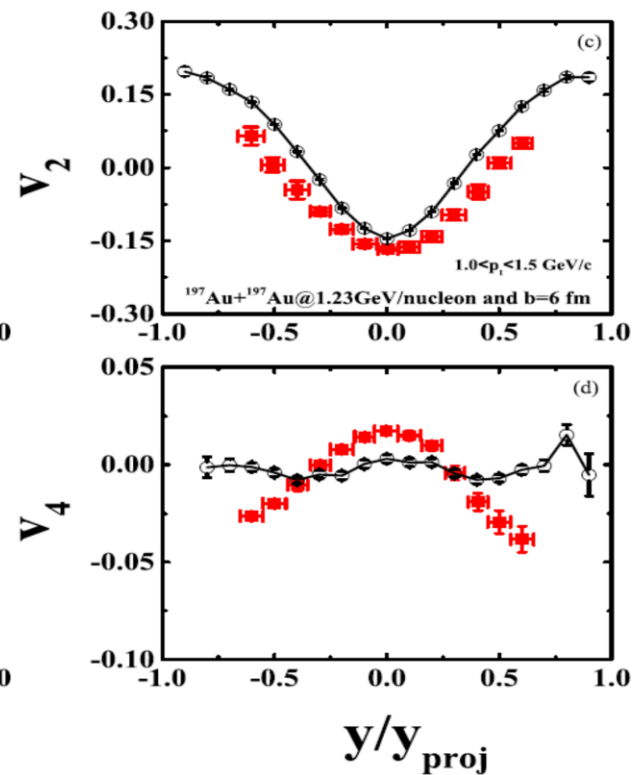
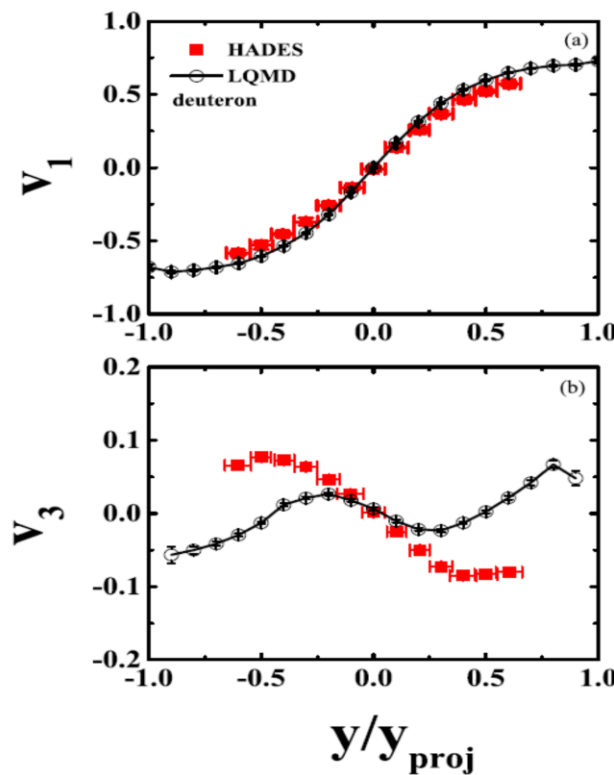
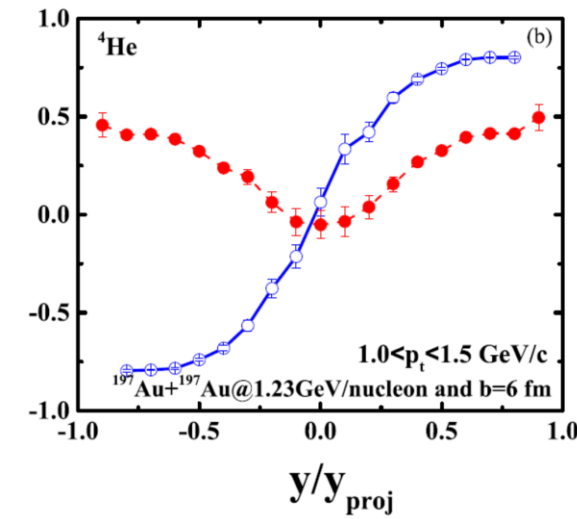
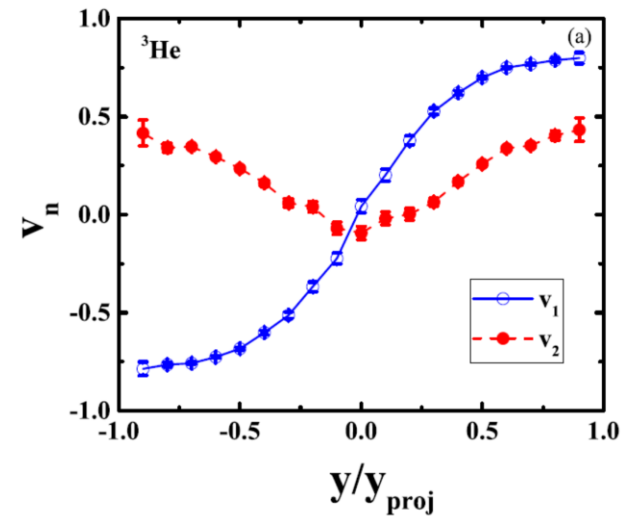
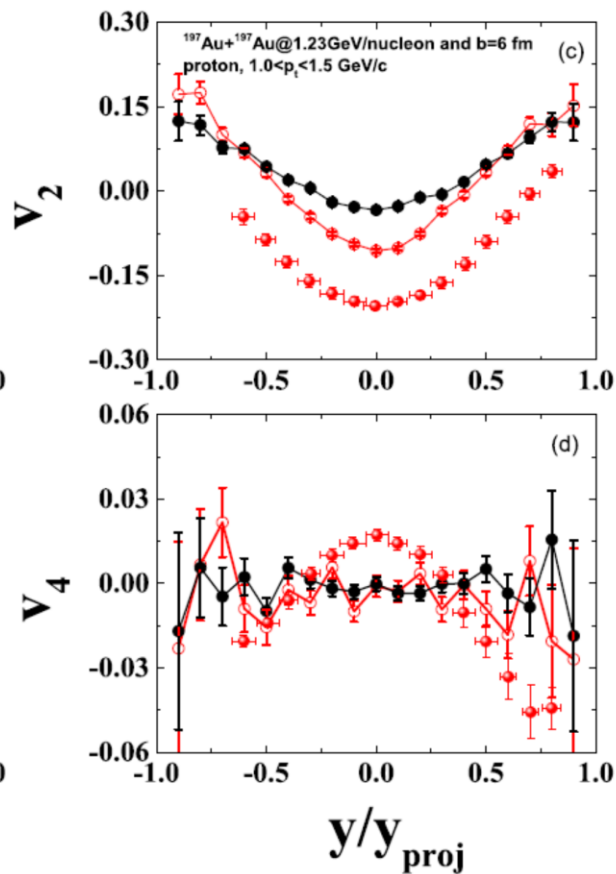
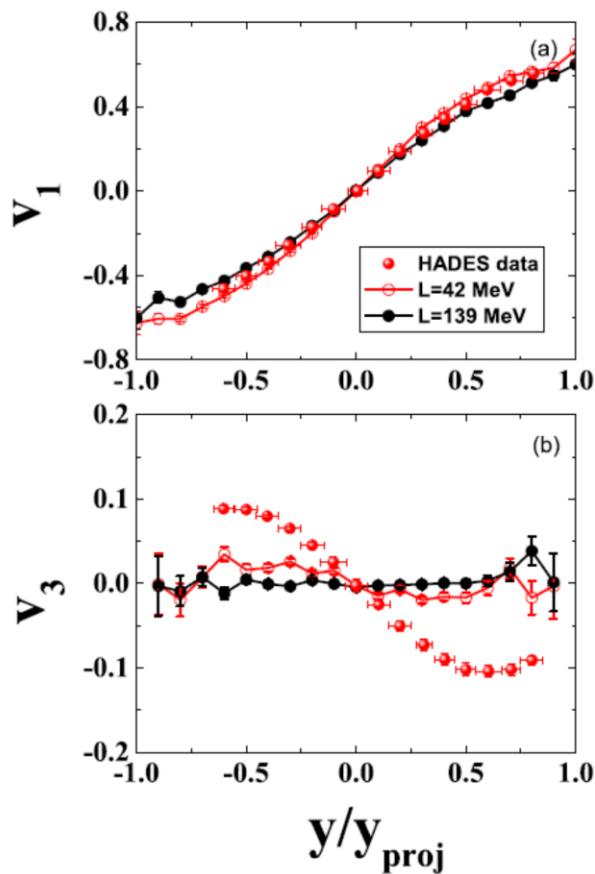


Symmetry energy and effective mass splitting (Ya-Fei Guo et al., Chinese Physics C 41 (2017) 104104)



Collective flows of clusters

Heng-Jin Liu, Hui-Gan Cheng, and Zhao-Qing Feng, PRC 108, 024614 (2023)

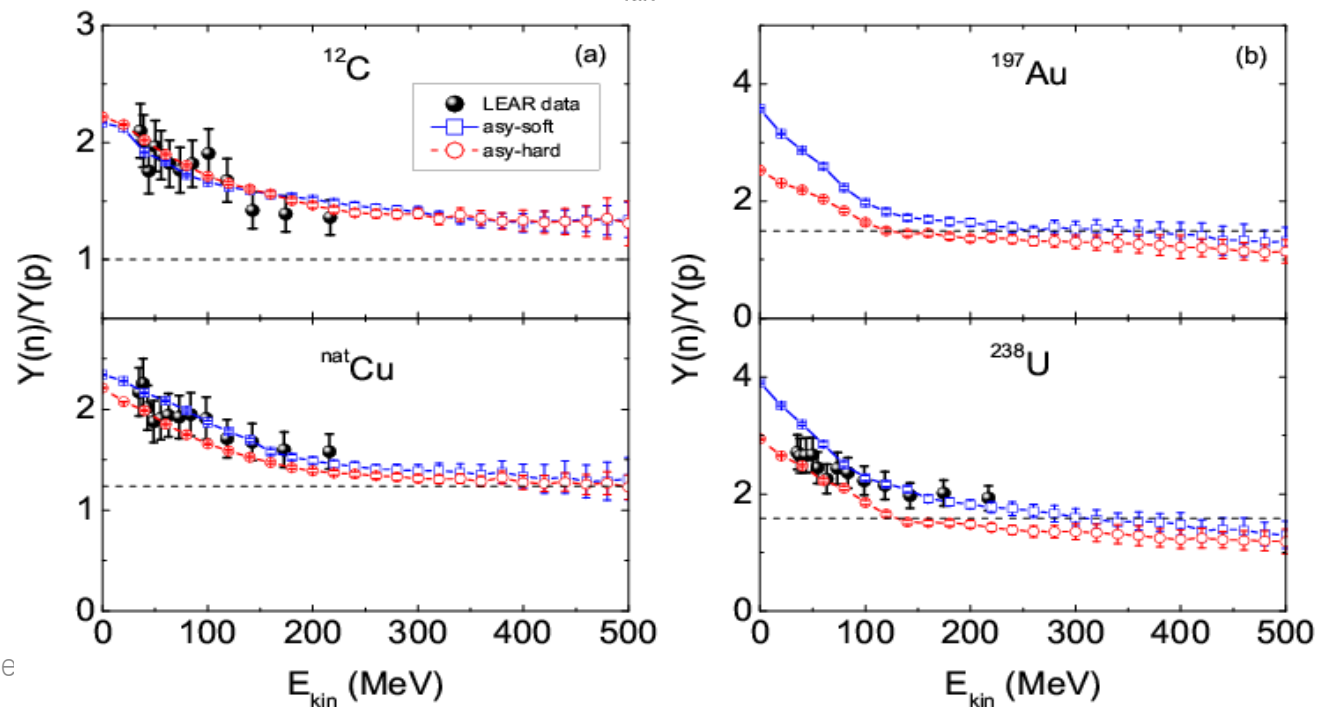
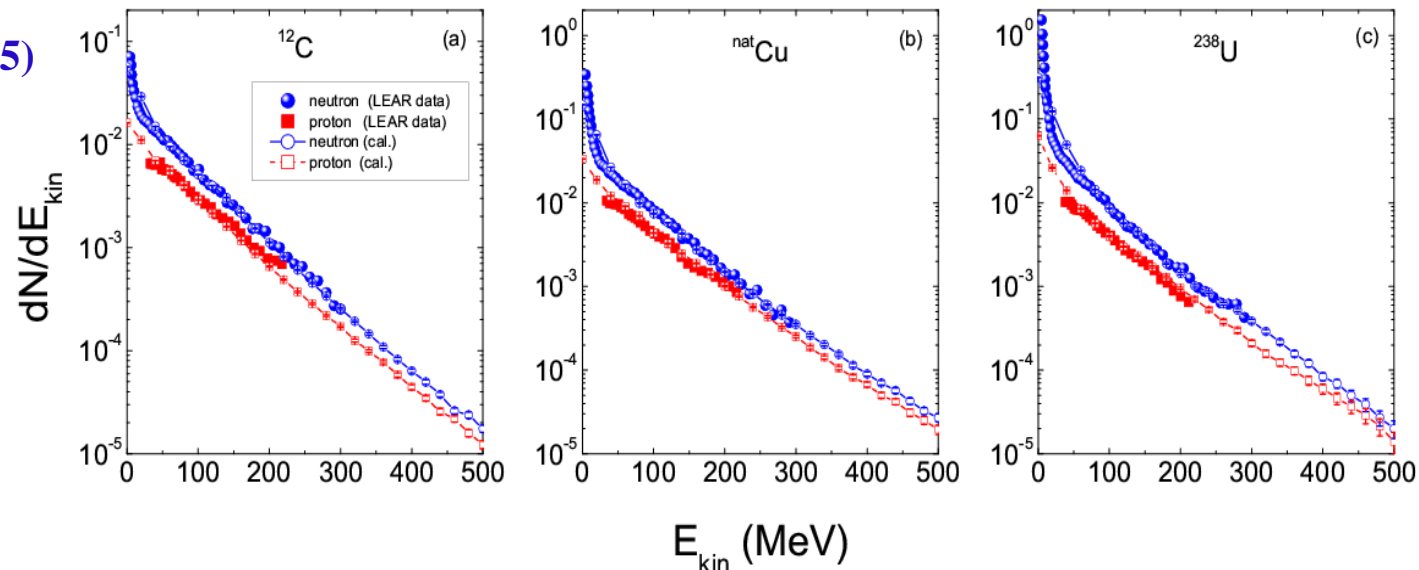
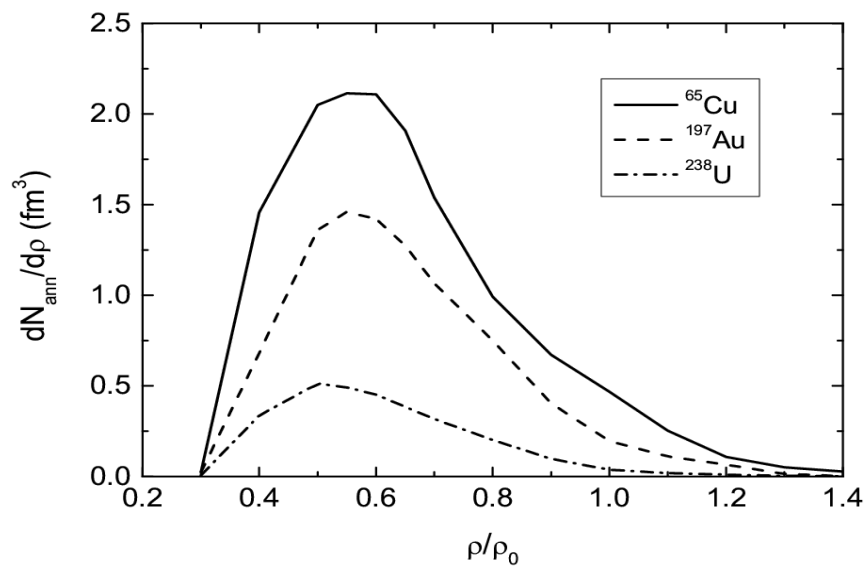
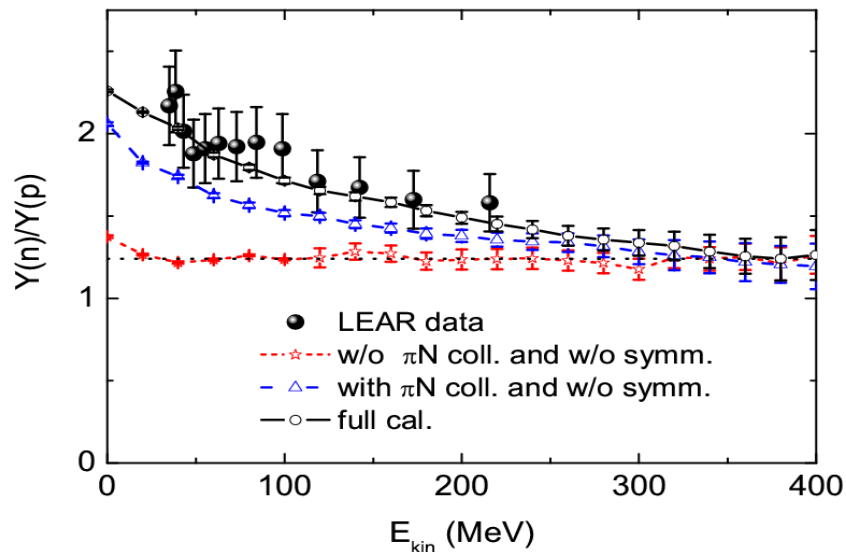


Isospin effect in low-energy antiproton-induced reactions

Slope parameter $L=53$ MeV

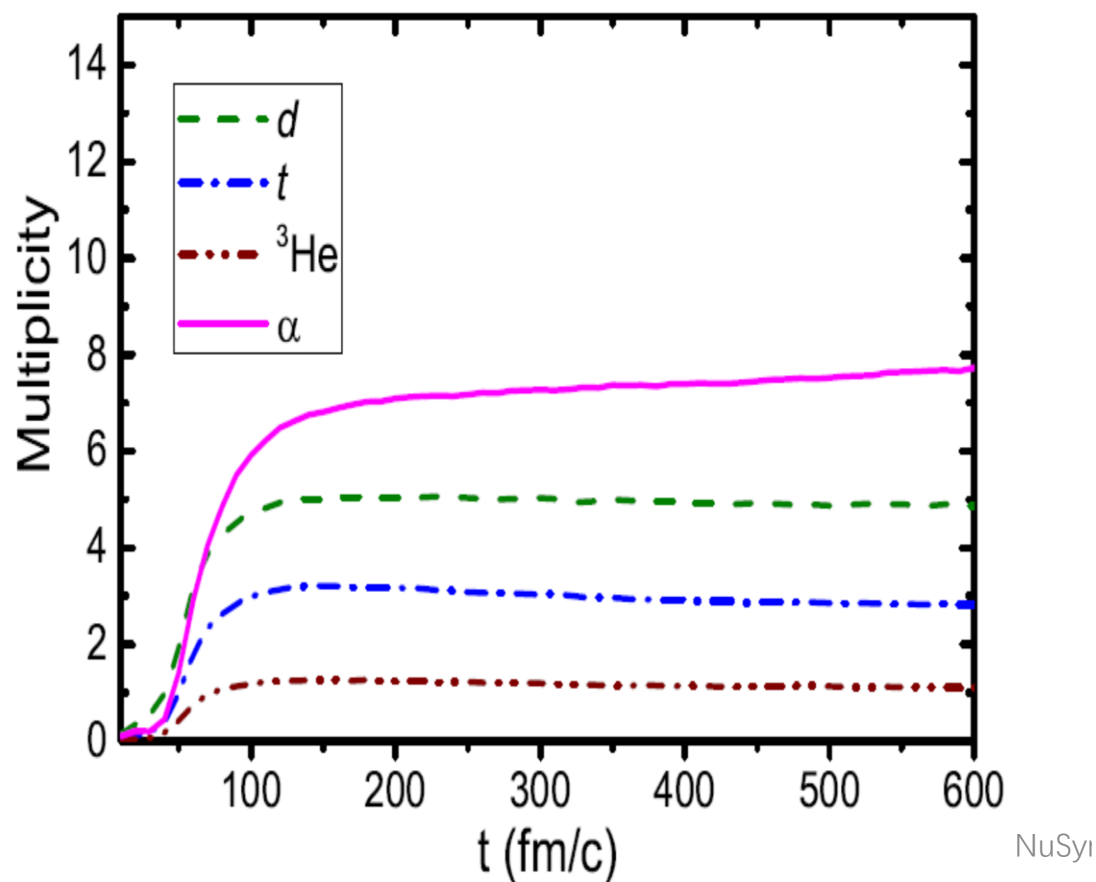
LEAR data: D. Polster et al., Phys. Rev. C 51, 1167 (1995)

(Z. Q. Feng, Phys. Rev. C 96, 034607 (2017))



Preequilibrium cluster production in heavy-ion collisions by including the multinucleon correlation, Mott effect, cluster scattering etc

$^{129}\text{Xe} + ^{118}\text{Sn}$ @ 50A MeV



NuSyI

Preequilibrium cluster emission and fragmentation reactions in heavy-ion collisions

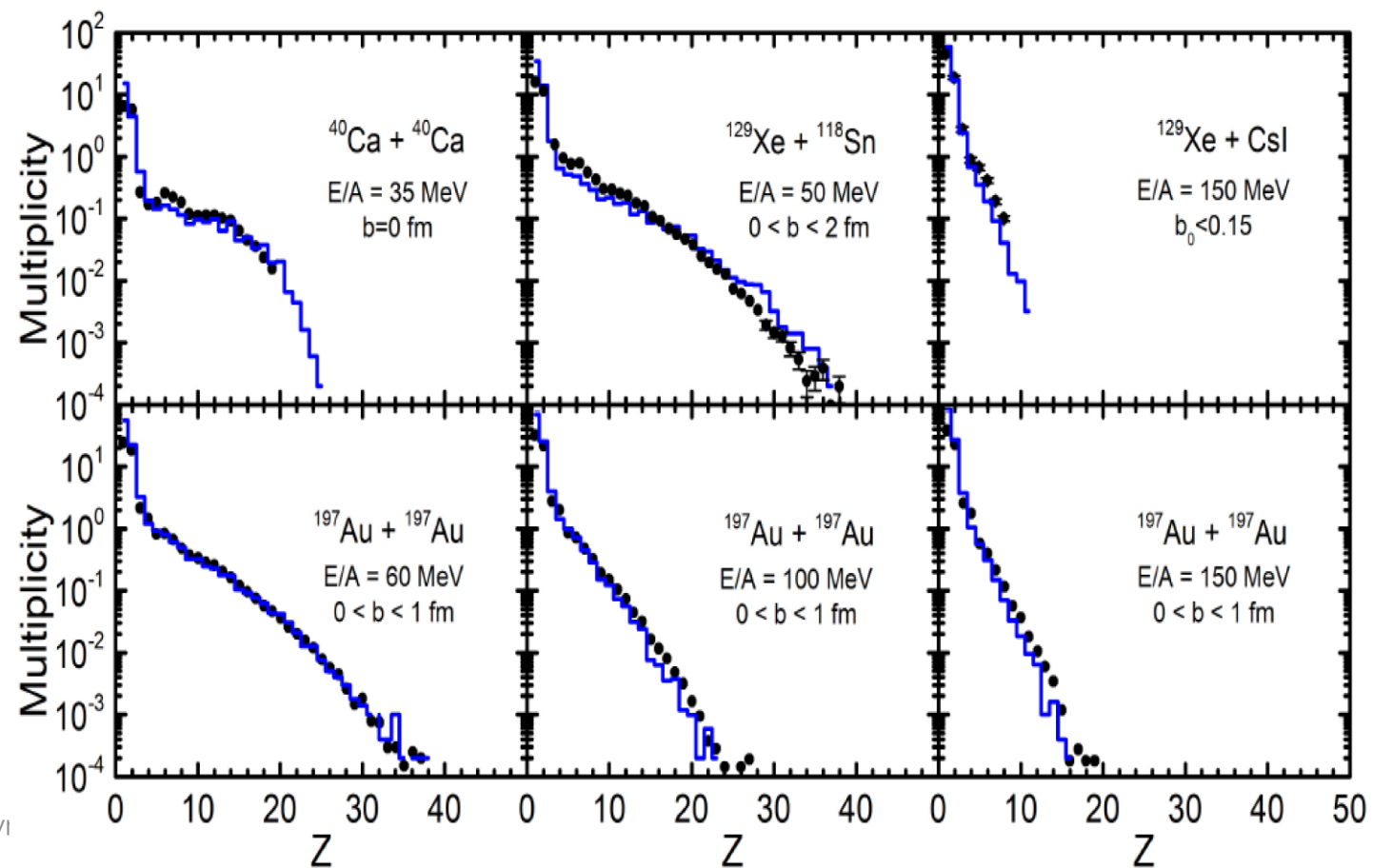
Hui-Gan Cheng and Zhao-Qing Feng*

School of Physics and Optoelectronics, South China University of Technology, Guangzhou 510640, China

(Dated: August 9, 2023)

A new method is proposed by incorporating the cluster correlation into the dynamical evolution of the standard quantum molecular dynamics (QMD) model. We demonstrate for the first time, the potential of the transport model in the description of light cluster production including the deuteron, triton, ^3He and α in fermi-energy heavy-ion collisions. Both the experimental multiplicities of light clusters and the charge distributions of heavier fragments are reasonably reproduced in the broad energy regime. The preequilibrium clusters via the multinucleon correlation dominate the yields in the fragmentation reactions, which are influenced by the multinucleon collisions, Mott effect, rescattering and rebounding between the nucleons and clusters. The enhancement of α production at the Fermi energies is caused by the larger binding energy and fermionic properties.

PACS number(s): 21.80.+a, 25.70.Pq, 25.75.-q

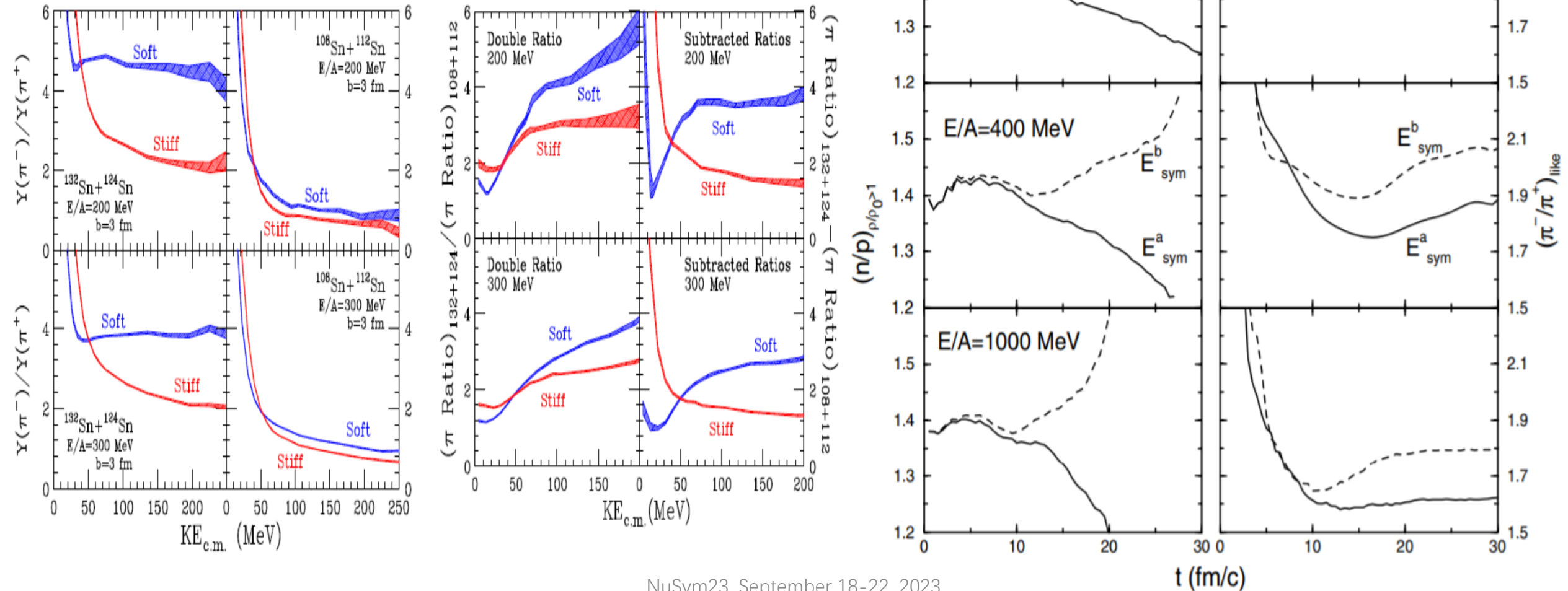


2. Pion production in heavy-ion collisions

Kinetic energy spectra of π^-/π^+ ratio

Bao-An Li, Phys. Rev. Lett. 88, 192701 (2002)

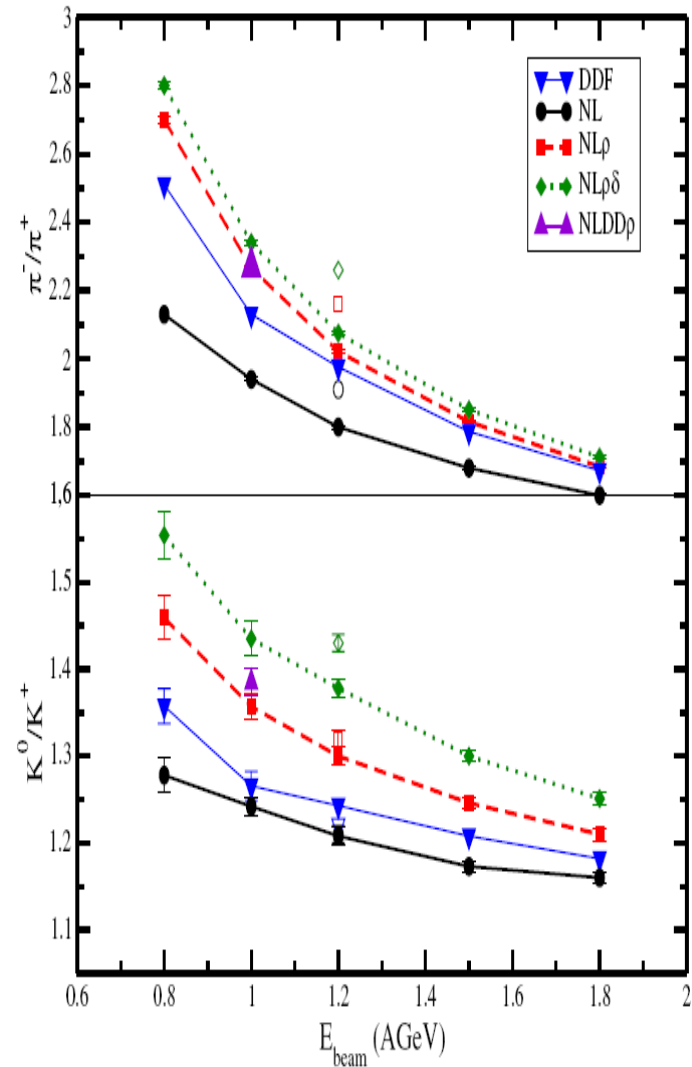
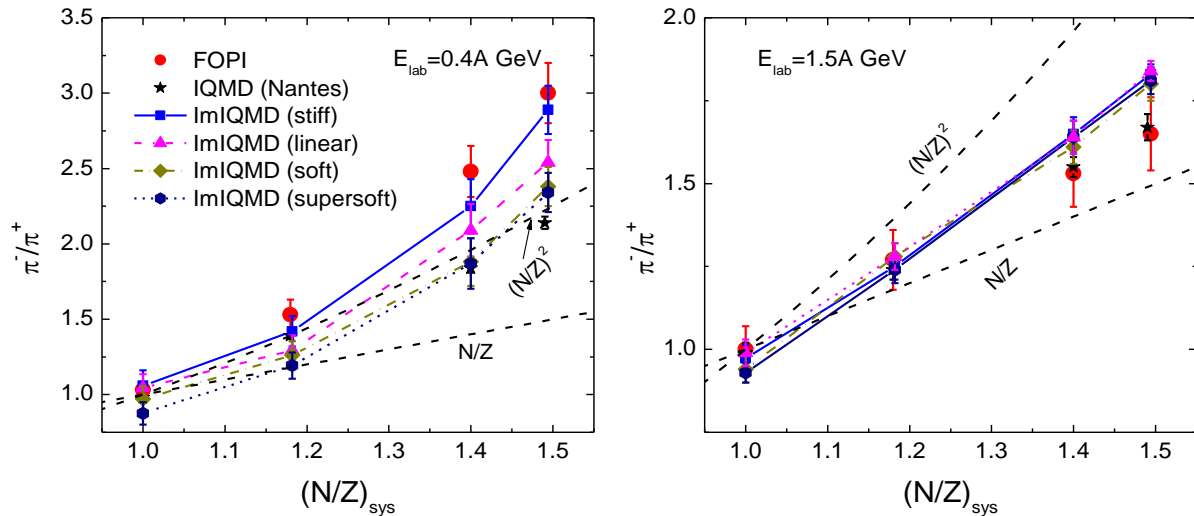
M. B. Tsang et al., Phys. Rev. C 95, 044614 (2017)



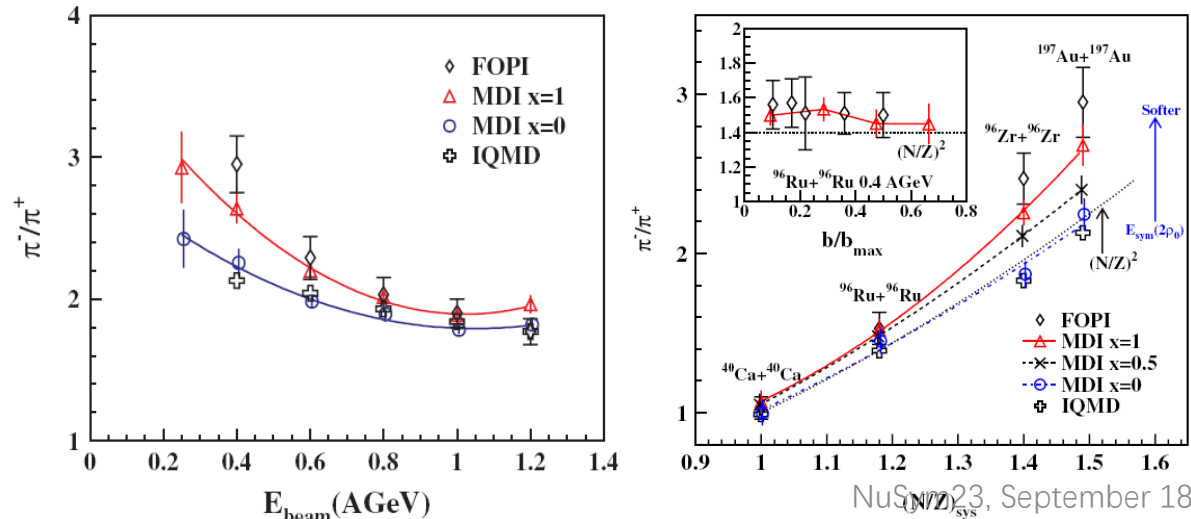
Pion production near threshold energies in heavy-ion collisions

LQMD: Phys. Lett. B 683 (2010) 140

RBUU: PRL97 (2006) 202301

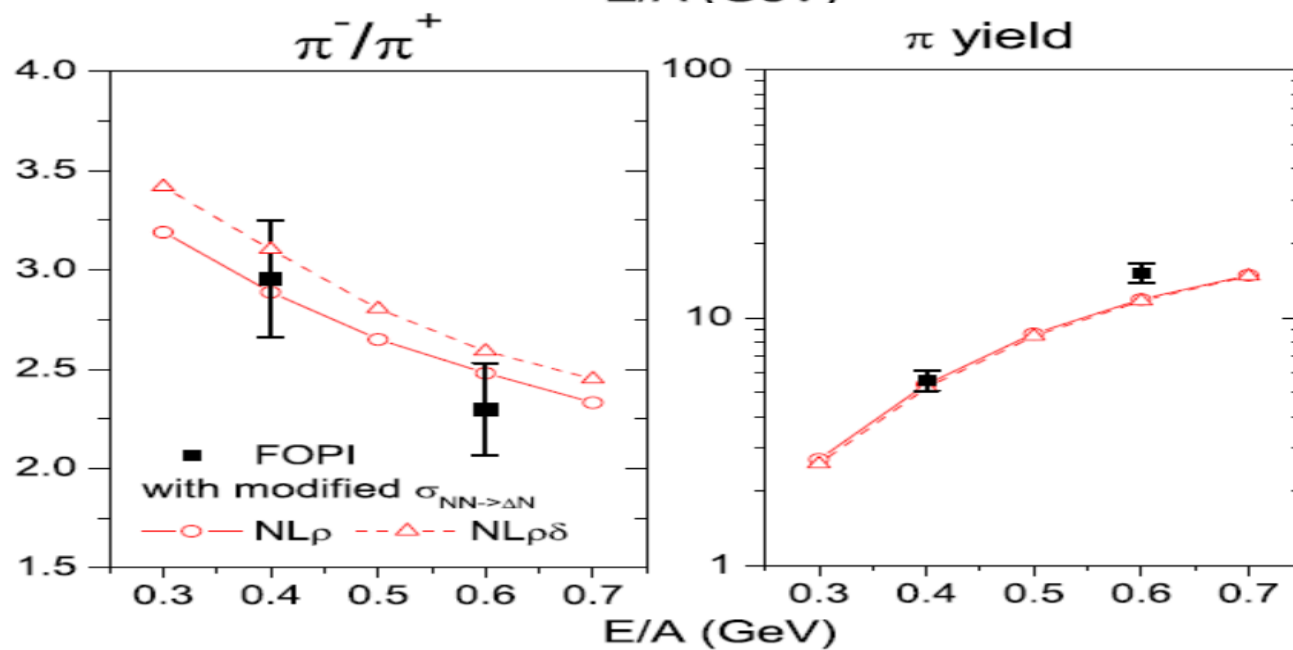
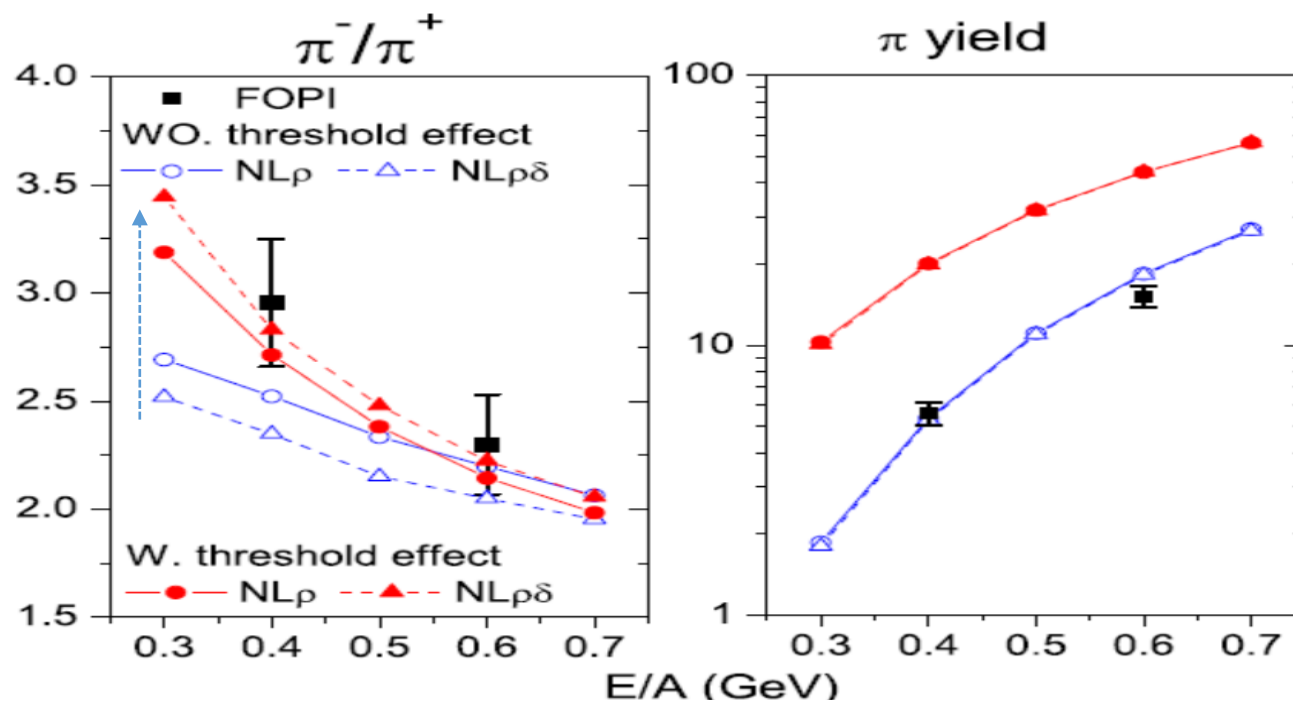
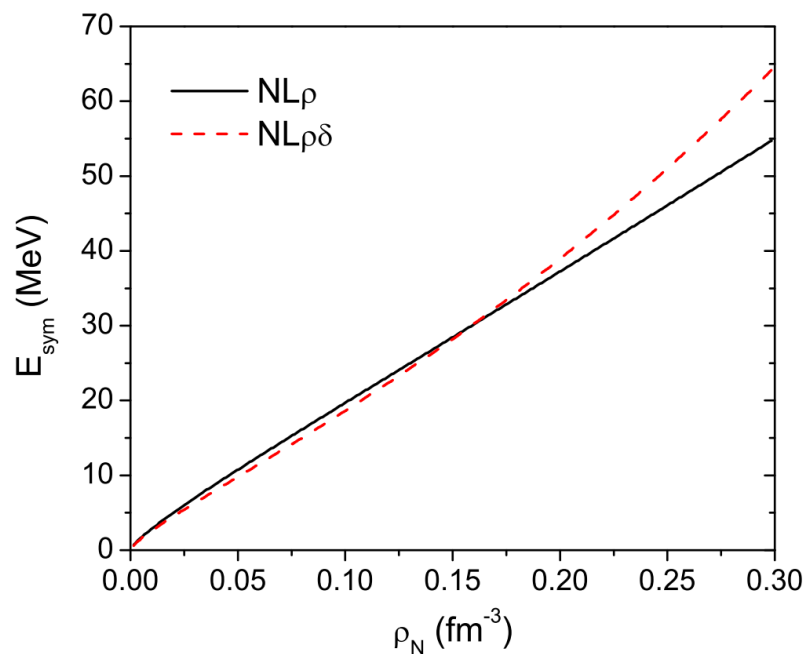


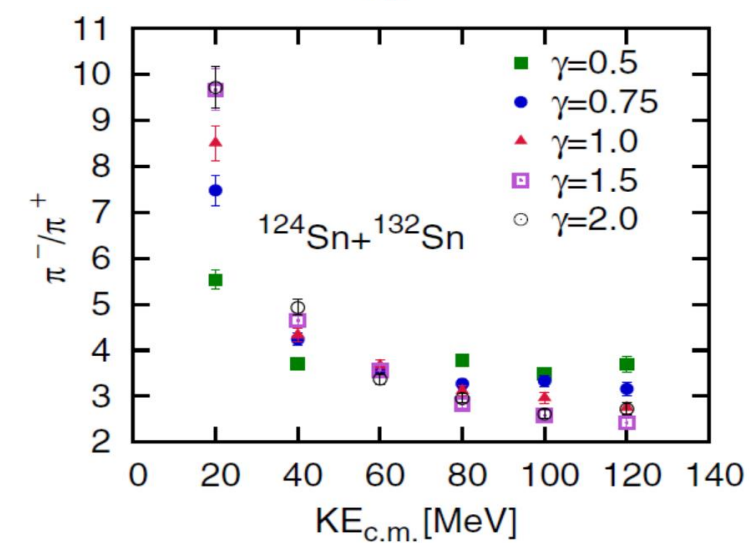
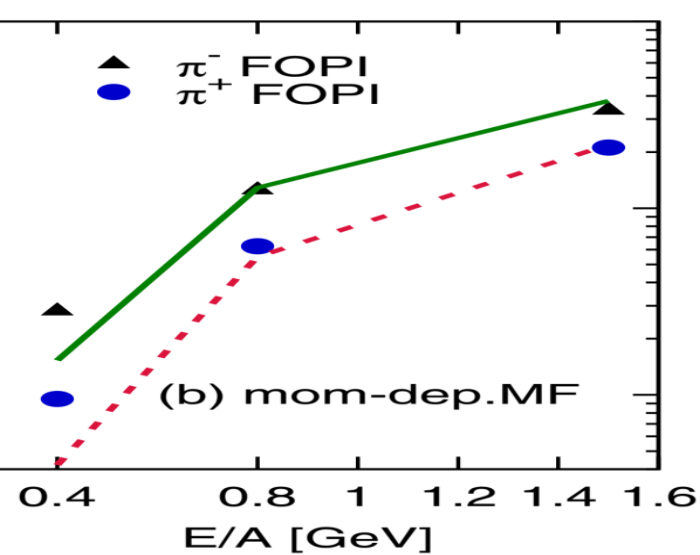
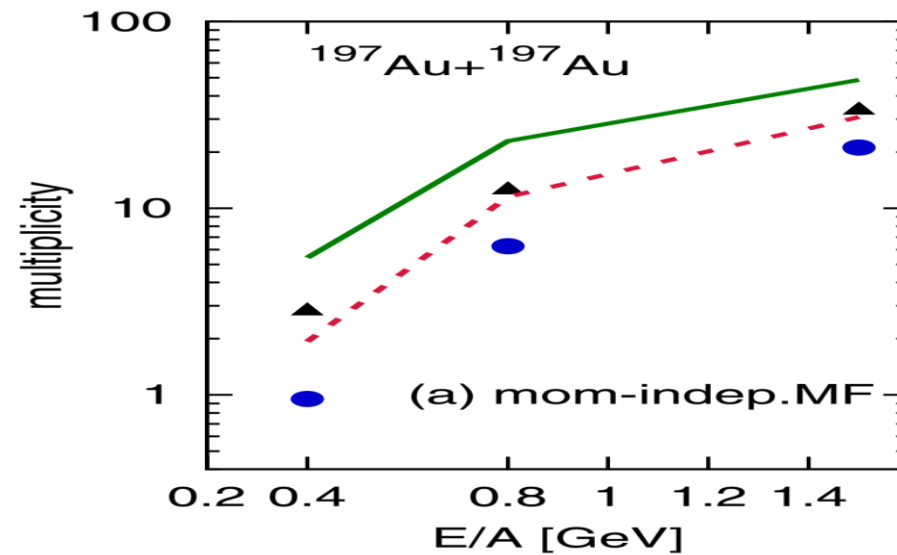
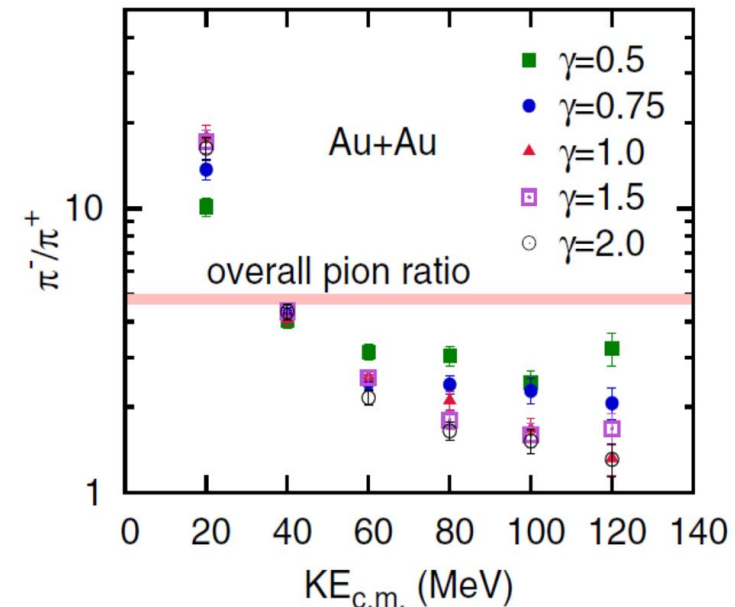
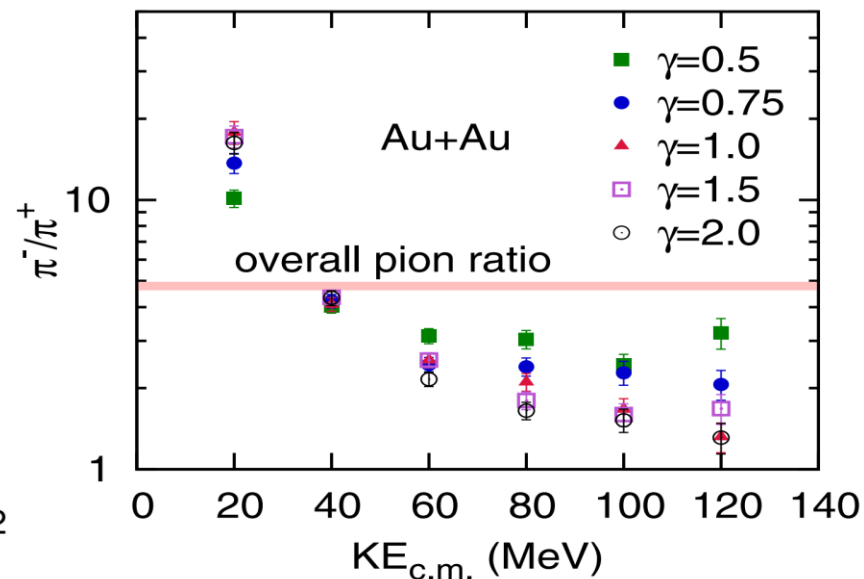
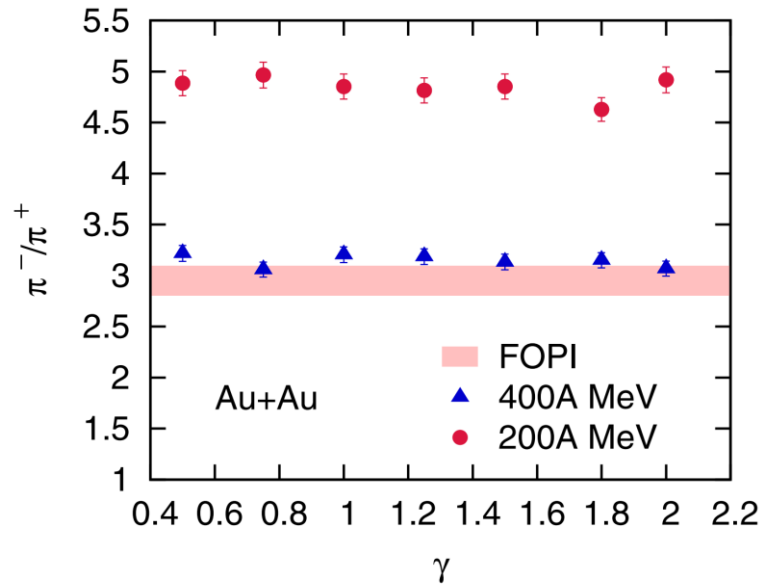
IBUU04: PRL102(2009)062502



Threshold effects of Δ production by the relativistic Vlasov-Uehling-Uhlenbeck (RVUU)

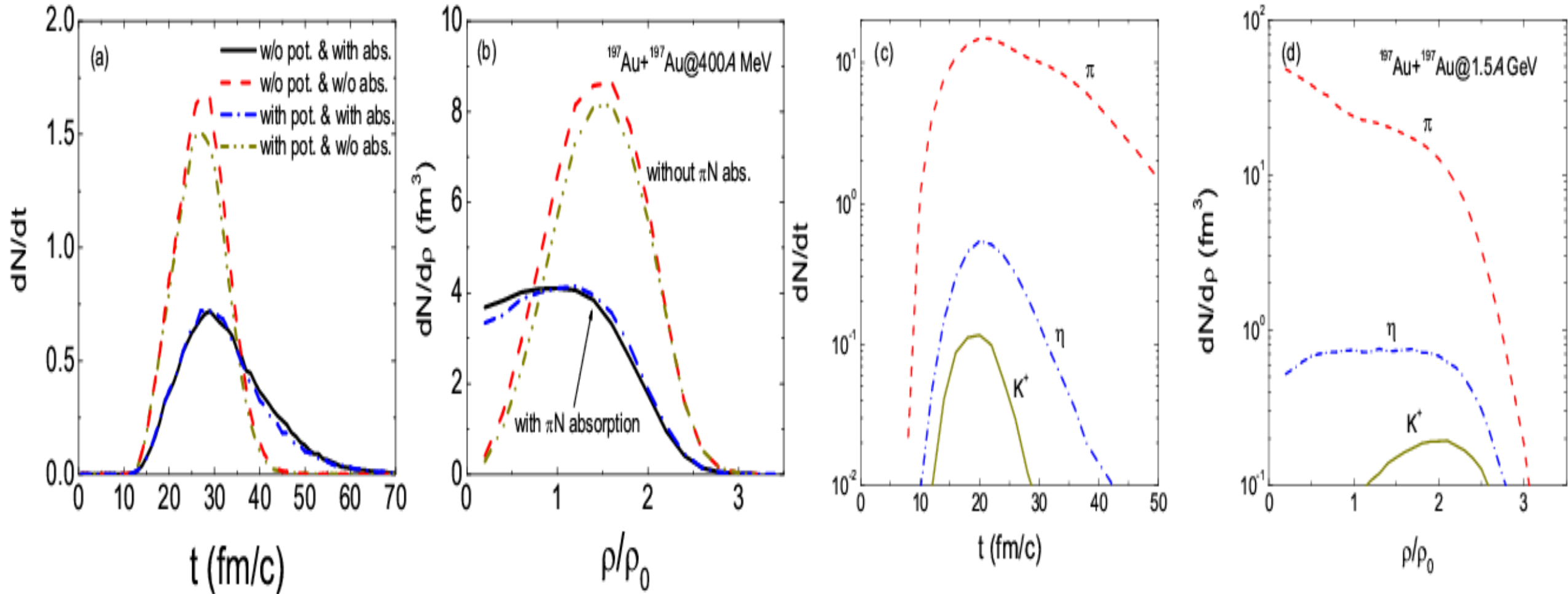
Taesoo Song, Che Ming Ko,
Phys. Rev. C 91, 014901 (2015)



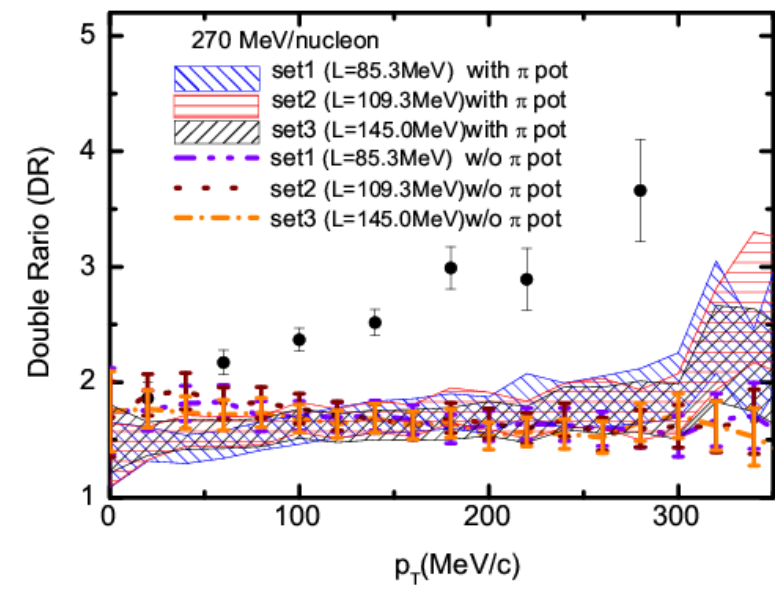
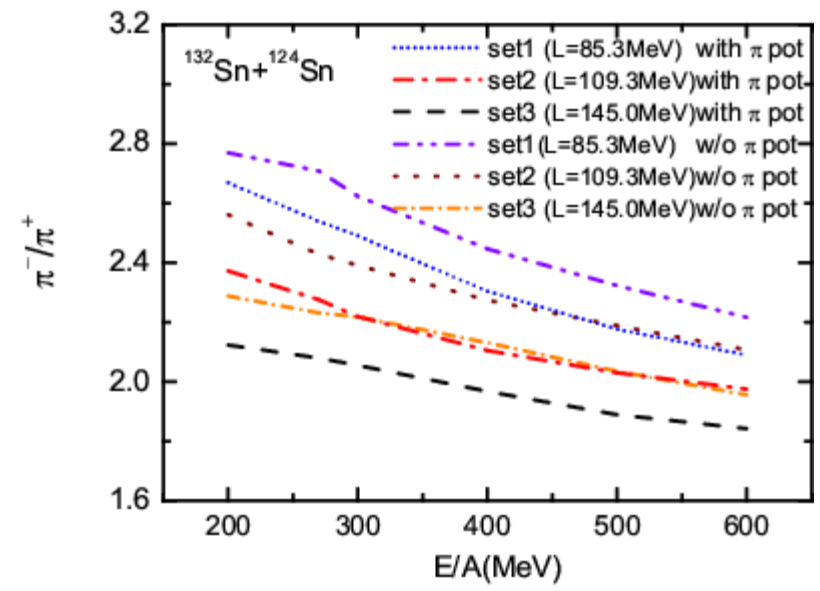
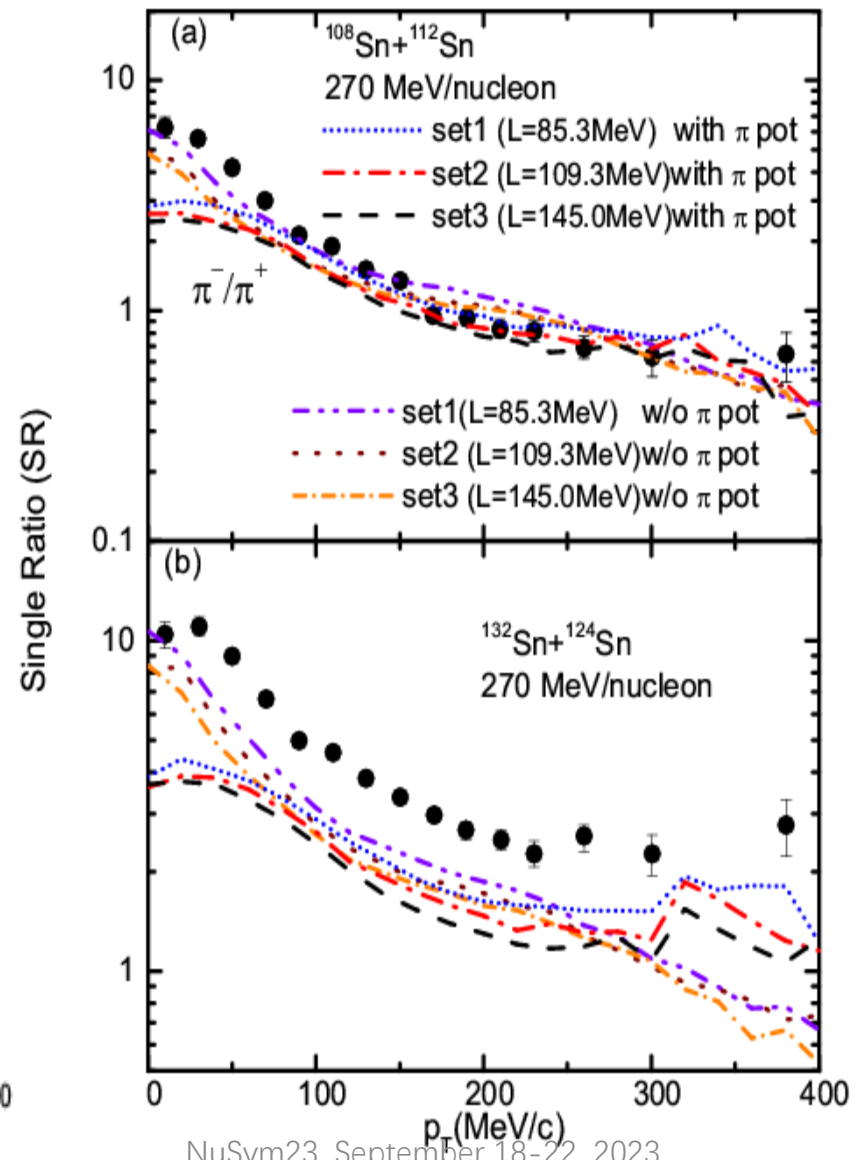
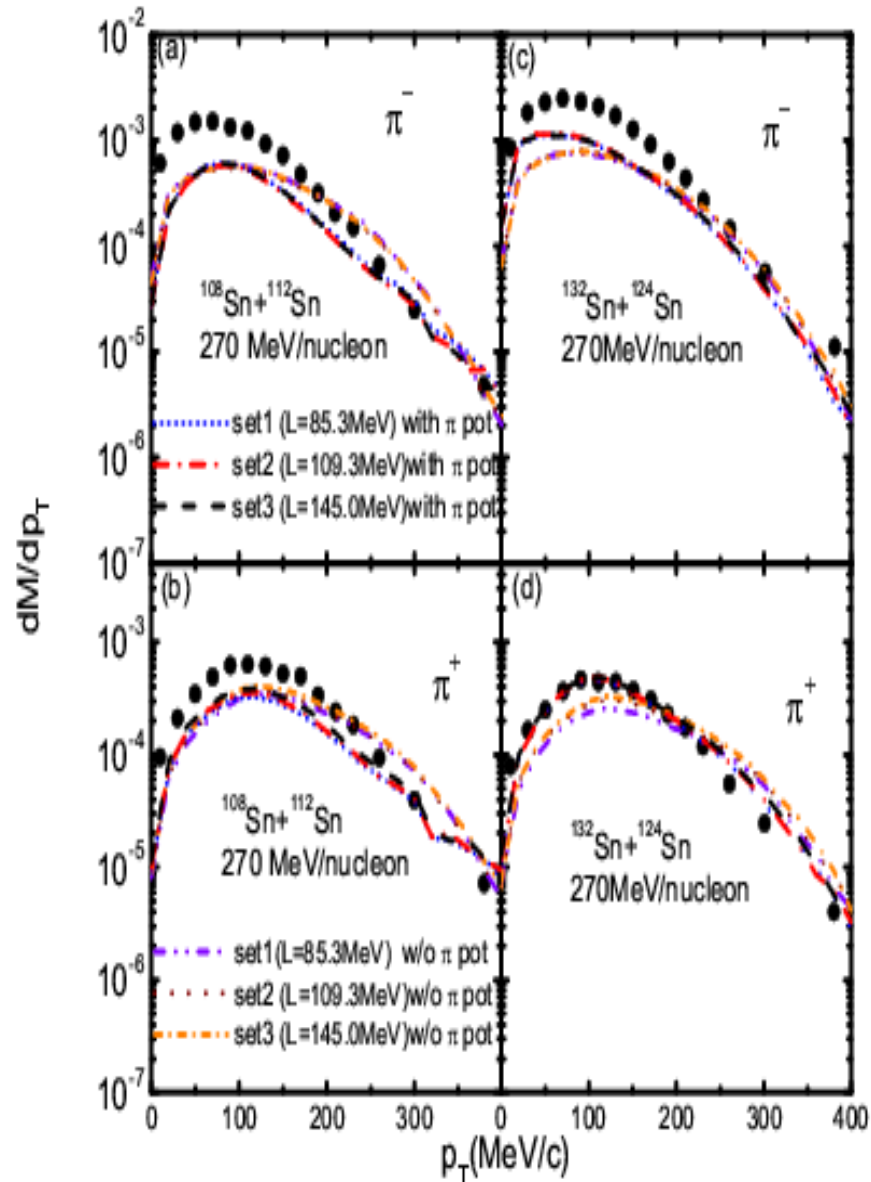


Temporal evolution of production rate and density profiles of particles in collisions of $^{197}\text{Au}+^{197}\text{Au}$

Zhao-Qing Feng, Nuclear Science and Techniques 29 (2018) 40. (Invited review) (arXiv:1802.10294)



Pion production in isotopic nuclear reactions by LQMD-RMF (Si-Na Wei, Zhao-Qing Feng, arXiv:2302.09984, PRC, **no threshold correction!**) The data are taken from J. Estee et al. (S π RIT Collaboration), Phys. Rev. Lett. 126, 162701 (2021).



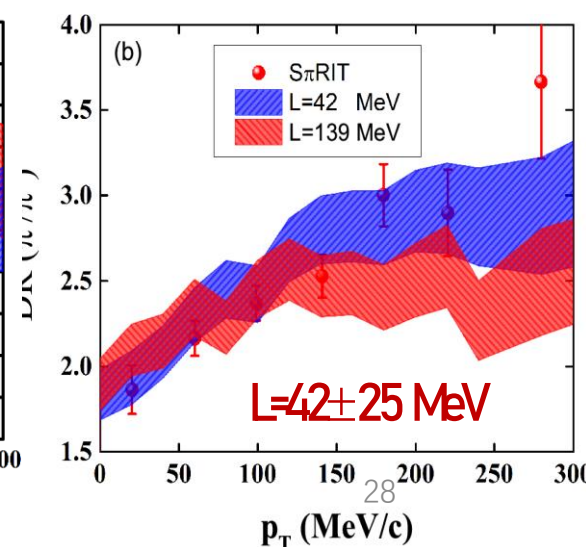
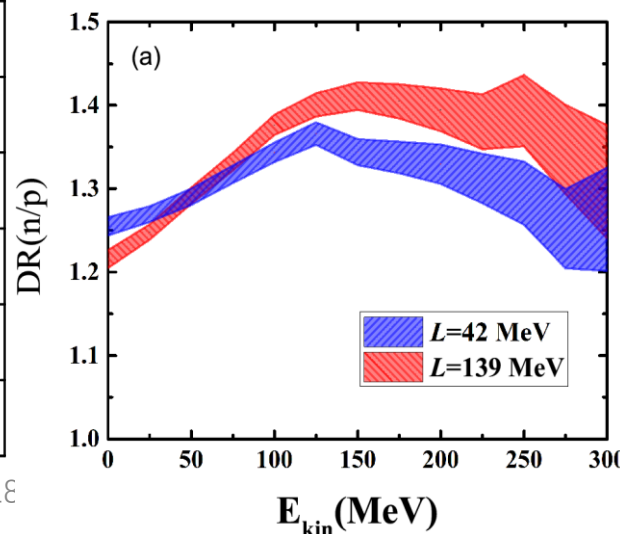
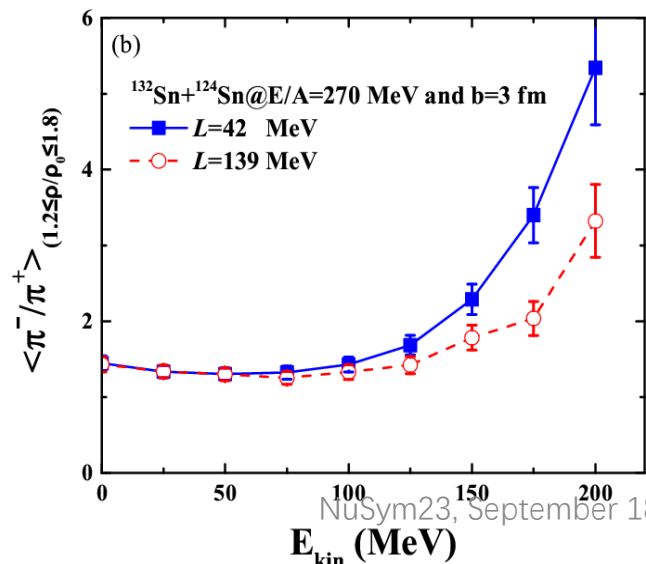
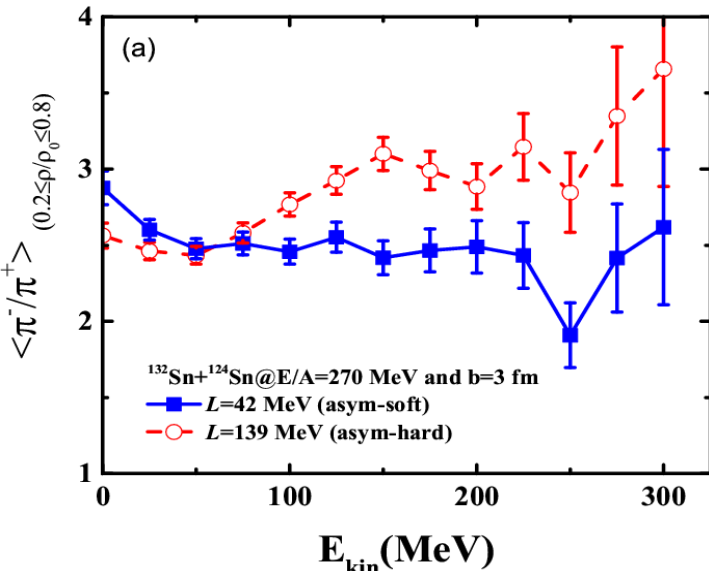
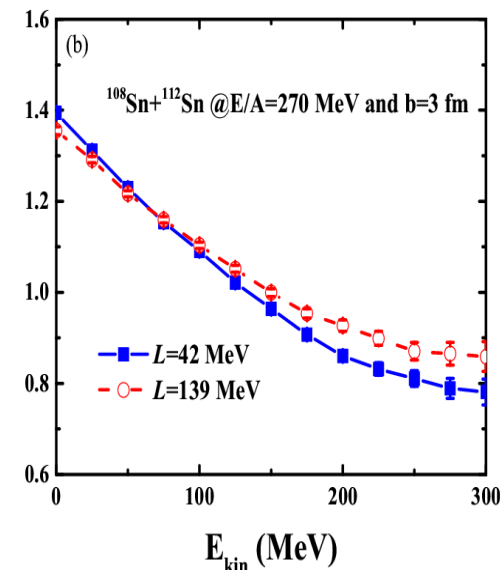
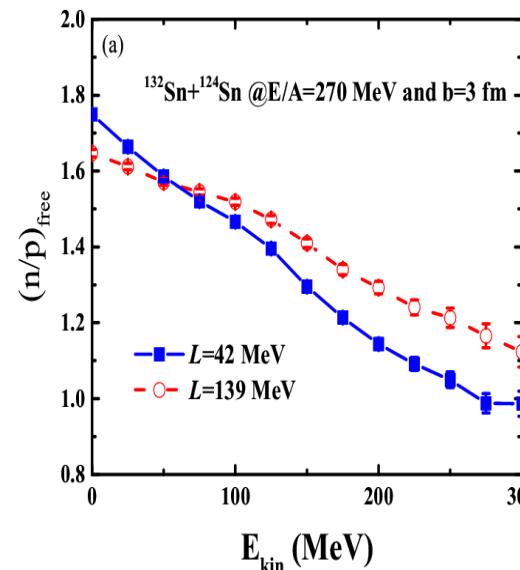
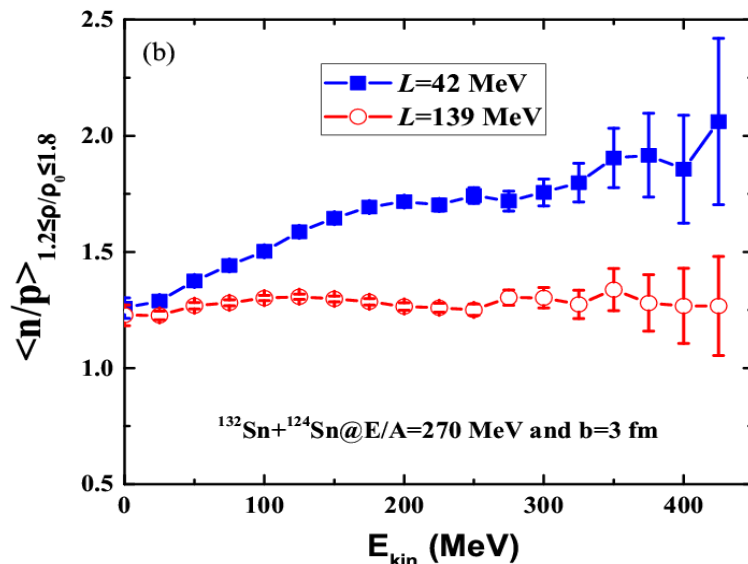
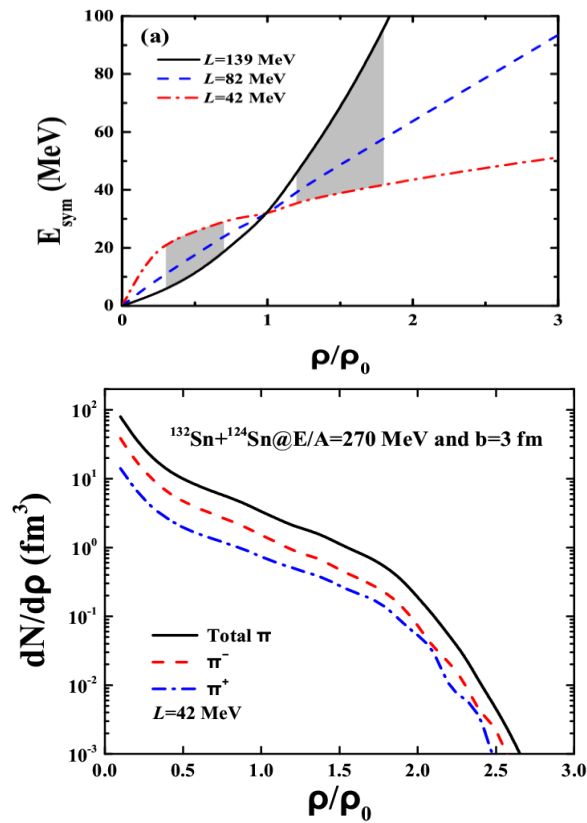
Shedding light on the pion production in heavy-ion collisions for constraining the high-density symmetry energy

LQMD-Skyrme, arXiv:2302.02131

Heng-Jin Liu, Hui-Gan Cheng, and Zhao-Qing Feng*

School of Physics and Optoelectronics, South China University of Technology, Guangzhou 510640, China

(Dated: March 19, 2023)



The pion production is overestimated by transport models!

Regular Article - Experimental Physics

Charged-pion production in Au + Au collisions at $\sqrt{s_{NN}} = 2.4$ GeV

HADES Collaboration

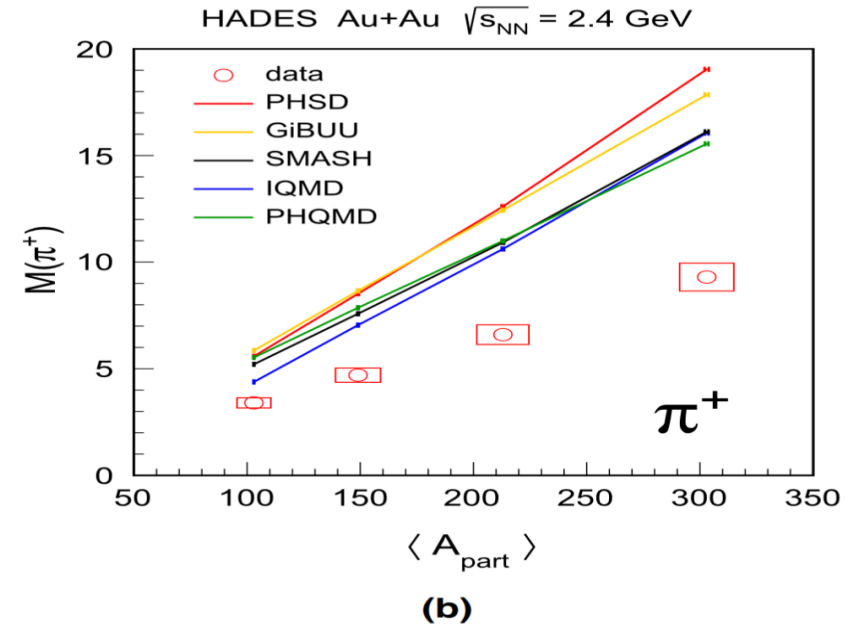
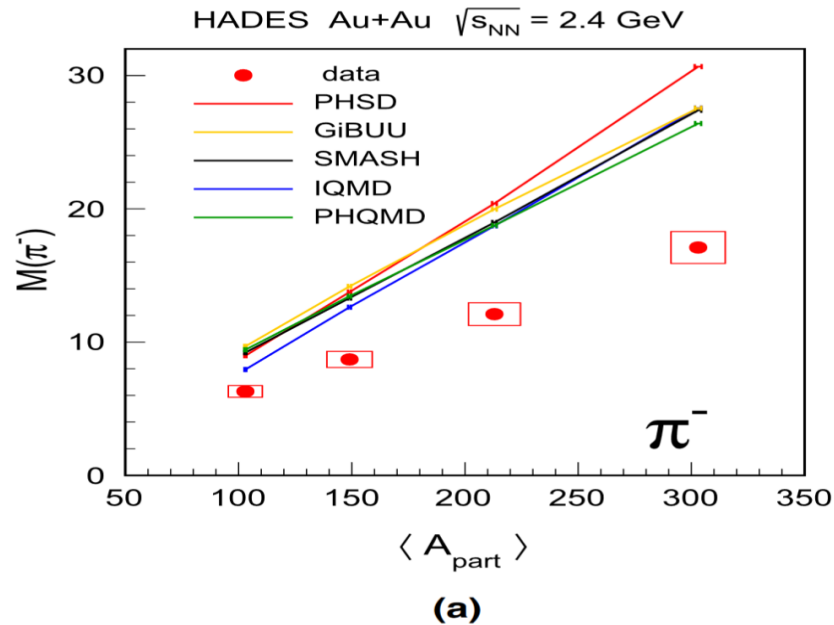
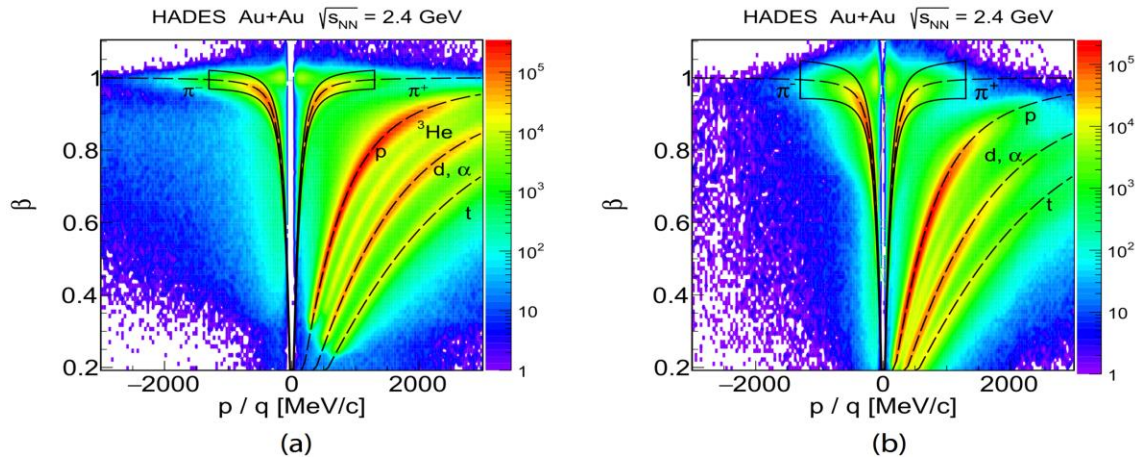


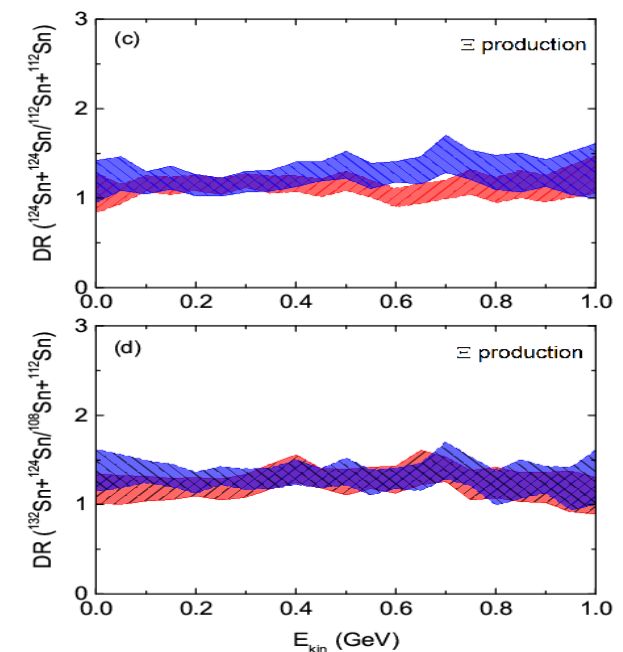
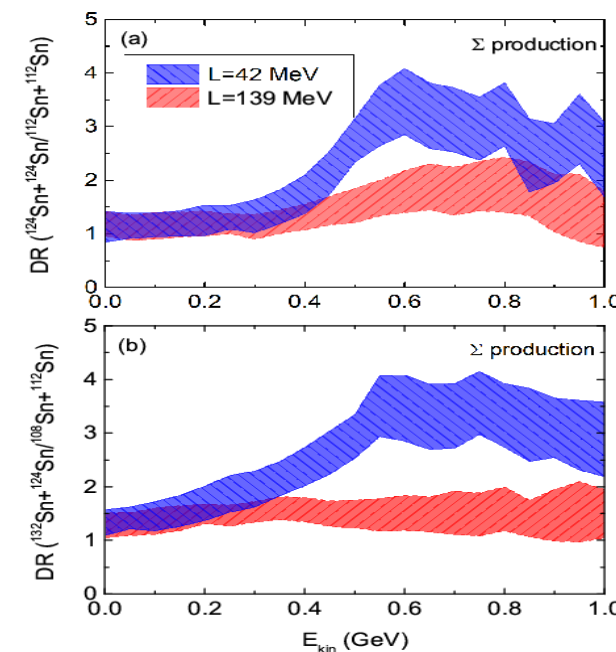
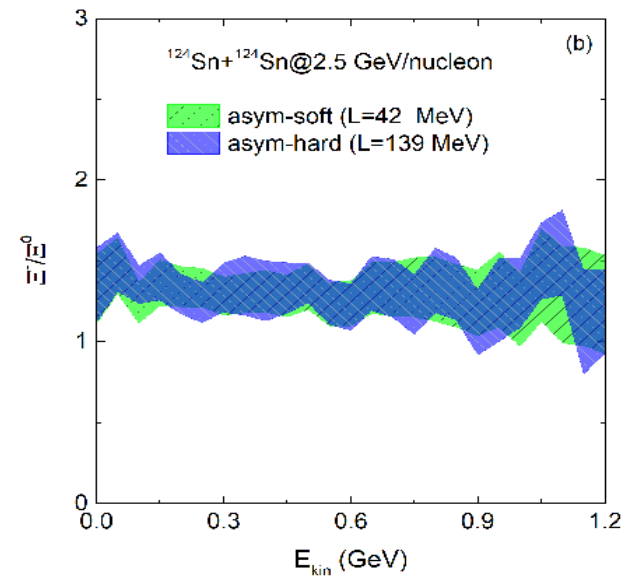
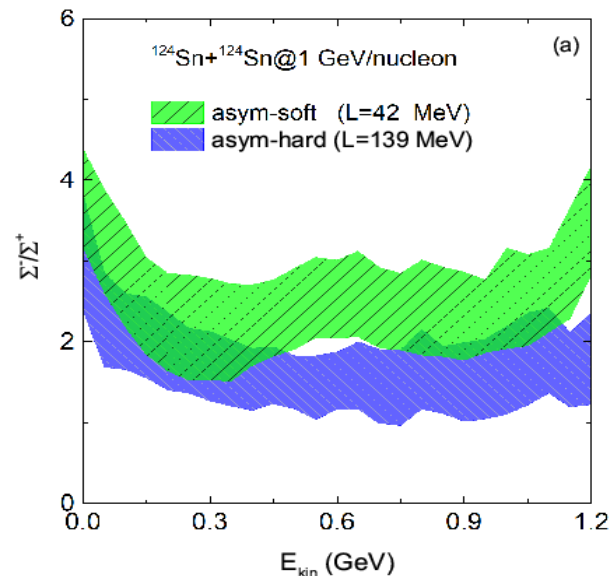
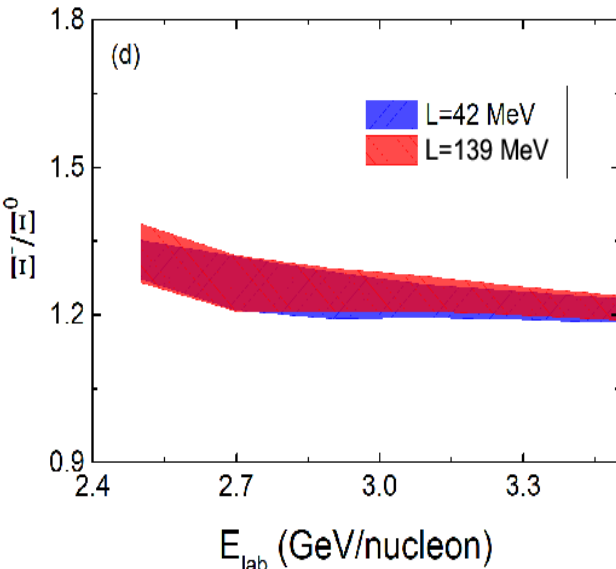
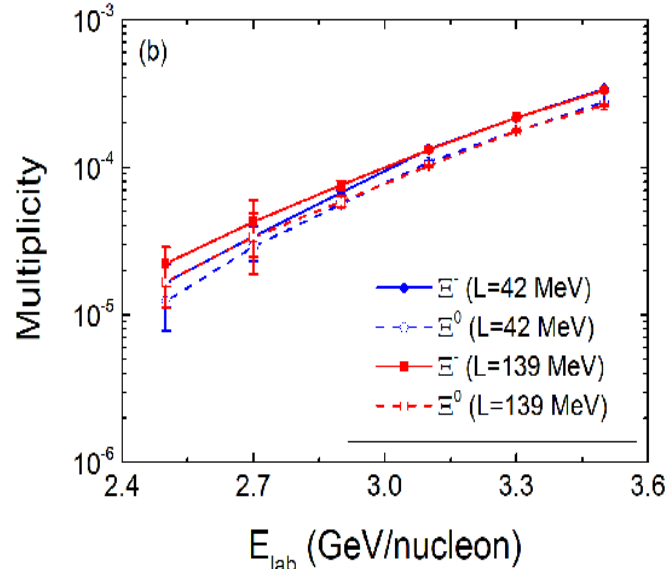
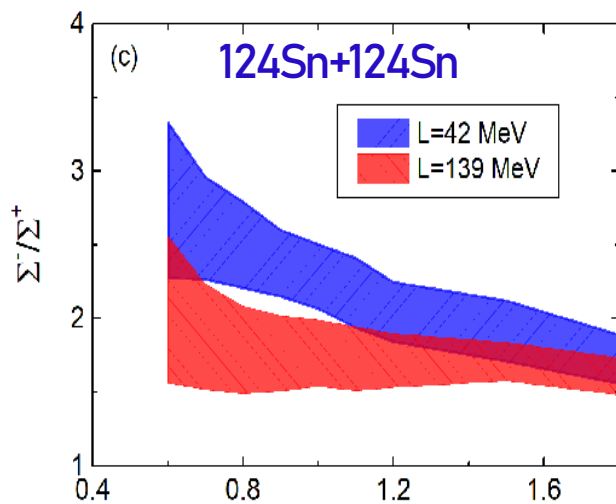
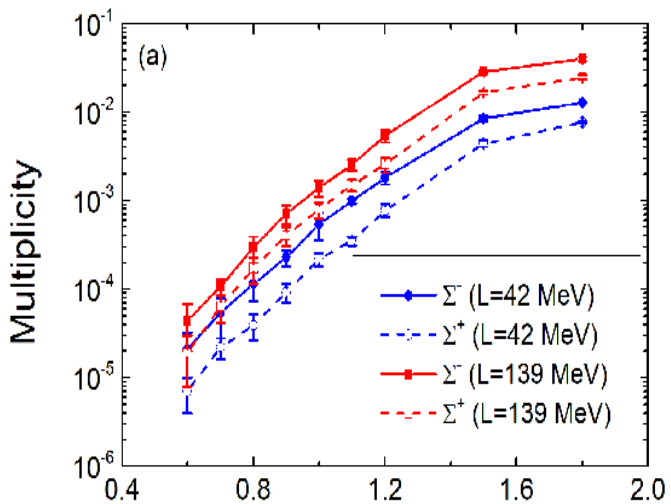
Fig. 7 Multiplicities of π^- (a) and π^+ (b) as a function of the mean number of participants $\langle A_{part} \rangle$. The vertical size of the open boxes stands for the systematic uncertainties due to the correction factors and extrapolations. The horizontal size of the open boxes indicates the error

on the mean number of participants (for details see [33]). Colored solid lines represent the results of various model calculations for π^- (π^+) (see Sect. 4)

3. Hyperon production in heavy-ion collisions

Zhao-Qing Feng, arXiv: 2303.04415, Phys. Lett. B (in press)

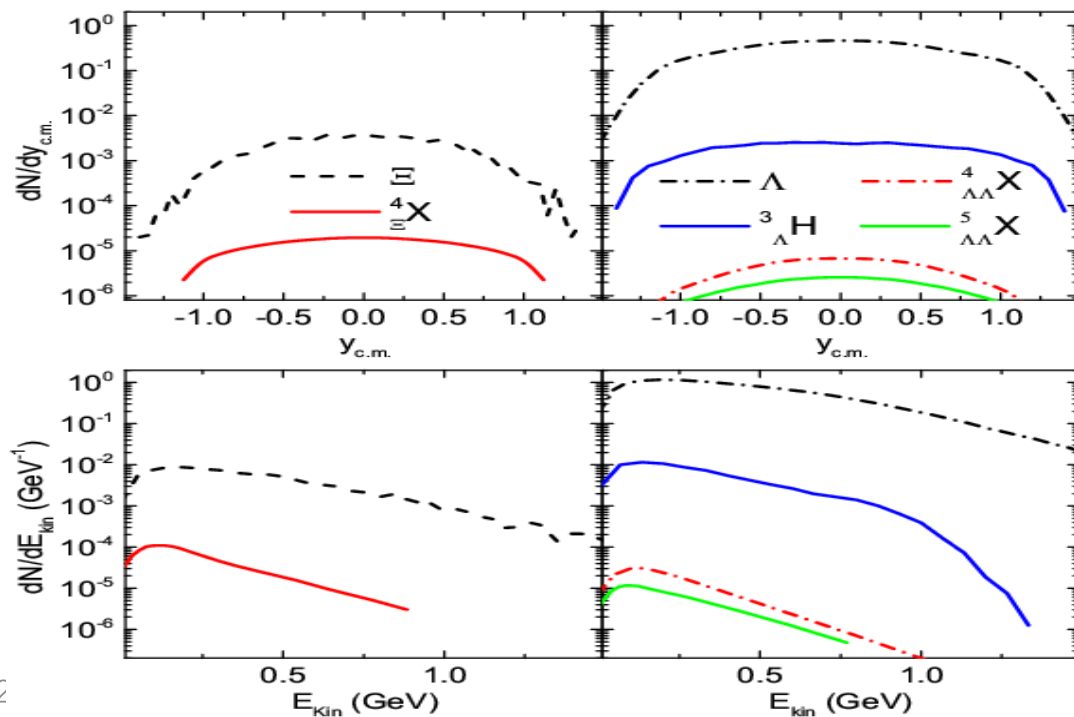
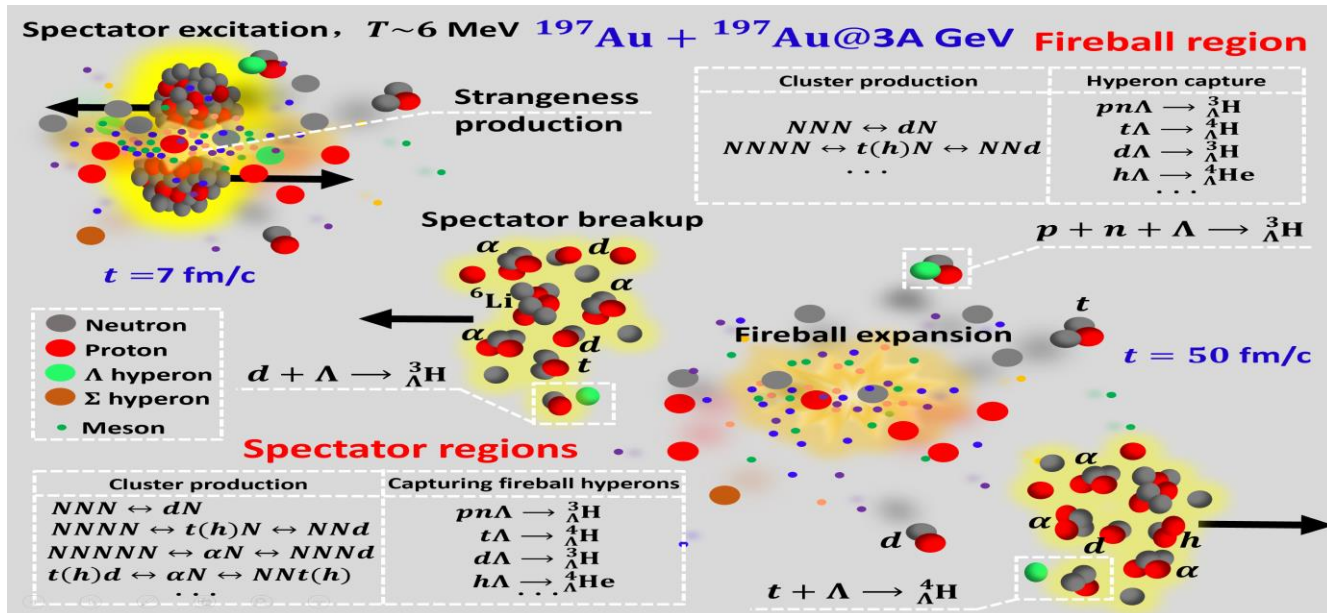
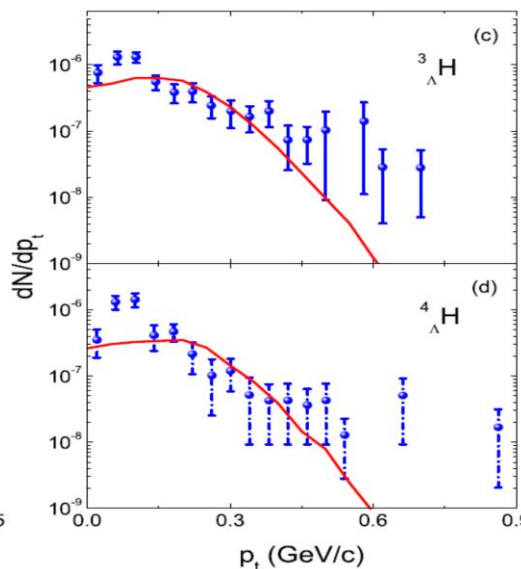
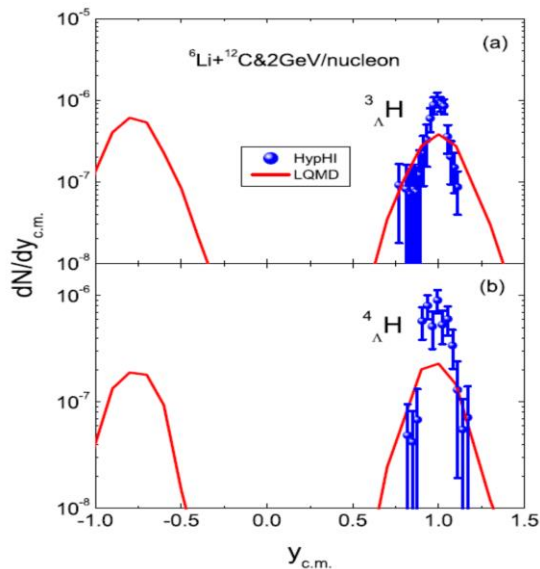
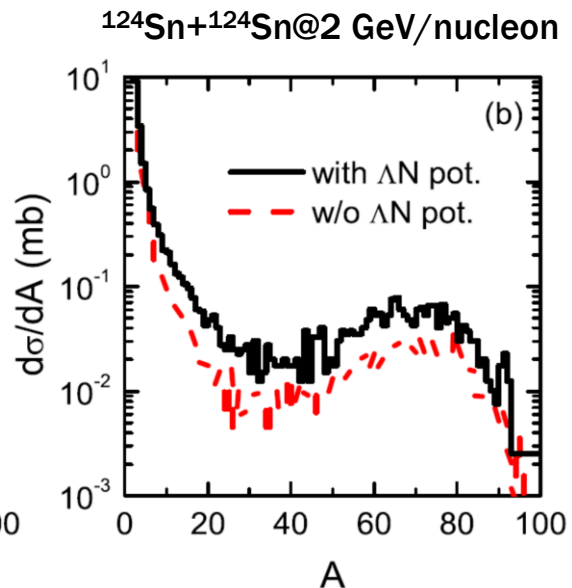
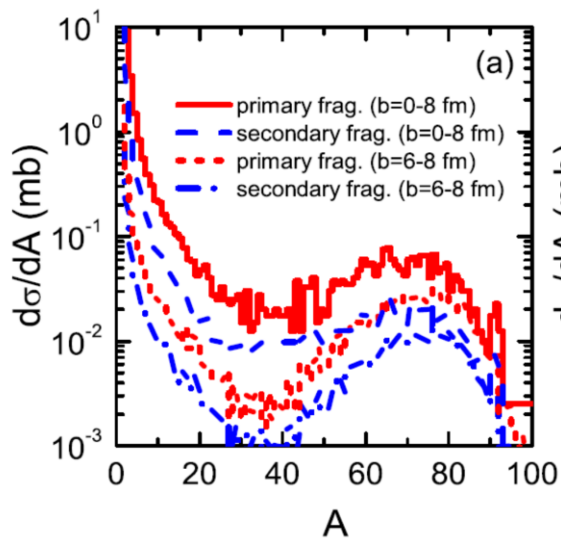
Σ^-/Σ^+ and Ξ^-/Ξ^0 for constraining the high-density SE



hypernuclide production in HICs

Z. Q. Feng, Phys. Rev. C 102, 044604 (2020)

H.G. Cheng, Z. Q. Feng, Phys. Lett. B 824, 136849 (2022)



IV. Summary and perspective

- A soft symmetry energy with the slope parameter of $L(\rho_0) = 42 \pm 25$ MeV by using the standard error analysis within the range of 1σ is obtained by analyzing the experimental data from the $S\pi$ RIT collaboration in reactions of $^{108}\text{Sn}+^{112}\text{Sn}$ and $^{132}\text{Sn}+^{124}\text{Sn}$ at 270 MeV/nucleon.
- The Σ^-/Σ^+ ratio depends on the stiffness of symmetry energy, in particular at the beam energy below the threshold value ($E_{\text{th}}=1.58$ GeV), i.e., the kinetic energy spectra of the single ratios, excitation functions and energy spectra of the double ratios in the isotopic reactions of $^{108}\text{Sn} + ^{112}\text{Sn}$, $^{112}\text{Sn} + ^{112}\text{Sn}$, $^{124}\text{Sn} + ^{124}\text{Sn}$ and $^{132}\text{Sn} + ^{124}\text{Sn}$. The double strangeness ratio Ξ^-/Ξ^0 weakly depends on the symmetry energy because of the hyperon-hyperon collision mainly contributing the Ξ production below the threshold energy ($E_{\text{th}} = 3.72$ GeV).
- Nuclear clusters and hypernuclear clusters for probing the high-density symmetry energy in the near future, $t/{}^3\text{He}$, ${}_{\Lambda}t/{}^3_{\Lambda}\text{He}$ etc.

!! key question: relation of cluster formation in heavy-ion collisions and pasta structure in neutron stars



Thank you for your attention